Lifetime measurements of states of ^{35}S, ^{36}S, ^{37}S, and ^{38}S using the AGATA γ-ray tracking spectrometer

L. Grocutt,[1,2] R. Chapman,[1,2,*] M. Bouhelal,[3] F. Haas,[4,5] A. Goasduff,[6] J. F. Smith,[1,2] R. S. Lubna,[7,8] S. Courtin,[4,5] D. Bazzacco,[9,10] T. Braunroth,[11] L. Capponi,[1,2,12] L. Corradi,[6] X. Derkx,[1,2] P. Desesquelles,[13,14] M. Doncel,[15,16] E. Fioretto,[6] A. Gottardo,[6] V. Liberati,[1,2] B. Melon,[17] D. Mengoni,[9,10] C. Michelagnoli,[18] T. Mijatović,[19] V. Modamio,[6] G. Montagnoli,[9,10] D. Montanari,[9,10] K. F. Mulholland,[1,2] D. R. Napoli,[6] C. M. Petrache,[20] A. Pipidis,[6] F. Recchia,[9,10] E. Sahin,[6,21] P. P. Singh,[22] A. M. Stefanini,[6] S. Szilner,[19] and J. J. Valiente-Dobón[6]

[1]*School of Computing, Engineering, and Physical Sciences, University of the West of Scotland, Paisley PA1 2BE, United Kingdom*
[2]*Scottish Universities Physics Alliance (SUPA), United Kingdom*
[3]*Laboratoire de Physique Appliquée et Théorique, Université Larbi Tébessi, Tébessa, Algeria*
[4]*IPHC, Université de Strasbourg, Strasbourg F-67037, France*
[5]*CNRS, UMR7178, Strasbourg F-67037, France*
[6]*Istituto Nazionale di Fisica Nucleare, Laboratori Nazionali di Legnaro, I-35020 Legnaro, Padova, Italy*
[7]*Department of Physics, Florida State University, Tallahassee, Florida 32306, USA*
[8]*TRIUMF, 4004 Wesbrook Mall, Vancouver, BC V6T 2A3, Canada*
[9]*Dipartimento di Fisica e Astronomia, Universitá degli Studi di Padova, I-35131 Padova, Italy*
[10]*Istituto Nazionale di Fisica Nucleare, Sezione di Padova, I-35131 Padova, Italy*
[11]*Institute für Kernphysik der Universitat zu Köln, D-50937 Köln, Germany*
[12]*Extreme Light Infrastructure Nuclear Physics/IFIN-HH, Bucharest-Magurele, RO-077125, Romania*
[13]*Centre des Sciences Nucléaires et des Sciences de la Matières (CSNSM), Université Paris-Sud, France*
[14]*CNRS-IN2P3, Université Paris-Saclay, Bâtiment 104, 15 rue Clemenceau, F91405 Orsay Cédex, France*
[15]*Laboratorio de Radiaciones Ionizantes, Universidad de Salamanca, E-37008 Salamanca, Spain*
[16]*Department of Physics, Oliver Lodge Laboratory, University of Liverpool, Liverpool L69 7ZE, United Kingdom*
[17]*Dipartimento di Fisica e Astronomia, Universitá di Firenze, IT-50019, Sesto Fiorentino (Firenze), Italy*
[18]*Institut Laue-Langevin, B.P. 156, F-38042 Grenoble Cédex 9, France*
[19]*Ruder Bošković Institute, Zagreb, Croatia*
[20]*IJCLab, Université Paris-Saclay, CNRS/IN2P3, Building 104, 91400 Orsay, France*
[21]*Department of Physics, University of Oslo, P.O. Box 1048, Blindern, N-0316 Oslo, Norway*
[22]*Department of Physics, Indian Institute of Technology Ropar, Rupnagar, Punjab 140 001, India*

(Received 22 February 2022; accepted 1 August 2022; published 16 August 2022)

Lifetimes or lifetime limits of a small number of excited states of the sulfur isotopes with mass numbers $A = 35$, 36, 37, and 38 have been measured using the differential recoil-distance method. The isotopes of sulfur were populated in binary grazing reactions initiated by a beam of ^{36}S ions of energy 225 MeV incident on a thin ^{208}Pb target which was mounted in the Cologne plunger apparatus. The combination of the PRISMA magnetic spectrometer and an early implementation of the AGATA γ-ray tracking array was used to detect γ rays in coincidence with projectile-like nuclear species. Lifetime measurements of populated states were measured within the range from about 1 to 100 ps. The number of states for which lifetime measurements or lifetime limits were possible was limited by statistics. For ^{35}S, the lifetime was determined for the first $1/2^+$ state at 1572 keV; the result is compared with a previous published lifetime value. The lifetime of the 3^- state of ^{36}S at 4193 keV was determined and compared with earlier measurements. No previous lifetime information exists for the (6^+) state at 6690 keV; a lifetime measurement with large associated error was made in the present work. For ^{37}S, the states for which lifetime limits were established were those at 646 keV with $J^\pi = 3/2^-$ and at 2776 keV with $J^\pi = 11/2^-$; there are no previously published lifetime values for excited states of ^{37}S. Finally, a lifetime limit was established for the $J^\pi = (6^+)$ state of ^{38}S at 3675 keV; no lifetime information exists for this state in the literature. Measured lifetime values were compared with the results of state-of-the-art shell-model calculations based on the PSDPF, SDPF-U, and FSU effective interactions. In addition, nuclear magnetic-dipole and electric-quadrupole moments, branching ratios, mixing ratios, and electromagnetic transition rates, where available, have been compared with shell-model values. The current work suffers from poor statistics; nevertheless, lifetime

*robert.chapman@uws.ac.uk

 ©2022 American Physical Society

values and limits have been possible, allowing a useful discussion of the ability of state-of-the-art shell-model calculations to reproduce the experimental results.

DOI: 10.1103/PhysRevC.106.024314

I. INTRODUCTION

The present paper is concerned with the measurement of lifetimes of excited states of nuclei in the *sd* shell near the $N = 20$ shell closure using the differential recoil distance method [1,2]. The nuclei of interest were populated in binary grazing reactions initiated by the interaction of 225-MeV ^{36}S ions with a thin target of ^{208}Pb. The nuclear species observed in the reaction have previously been studied in an experiment carried out at the INFN Legnaro National Laboratory, Italy, using the same beam-target combination at a beam energy of 215 MeV, the energy of the ^{36}S ions at the center of the ^{208}Pb target in the present experiment. In the earlier work, the combination of PRISMA [3,4], a large solid angle magnetic spectrometer to identify the projectile-like nuclear species, and CLARA [5], an array of escape-suppressed Ge γ-ray detectors to measure the γ-ray decay of the populated levels, was used. In relation to the isotopes of sulfur, the previous published works from the experiment have involved studies of the isotopes ^{37}S [6], ^{39}S [7], ^{40}S [8], and ^{41}S [9]. In addition, the level structures of other populated isotopes of sulfur were investigated [10]. The earlier studies were mainly concerned with the role of negative-parity intruder orbitals in the structure of neutron-rich nuclei on the periphery of the island of inversion, which is centered on ^{32}Mg, and on the description of such nuclei using state-of-the-art shell-model calculations [11].

The spectroscopy and electromagnetic decay properties of the isotopes of sulfur have been the subject of many studies over recent years. The results reveal a rich tapestry of nuclear structure phenomena. While the work reported here is concerned with moderately neutron-rich isotopes which are difficult to reach with the more conventional fusion-evaporation reactions using stable projectiles, such reactions have been employed in investigations of the lighter isotopes of sulfur. A study of the more neutron-rich sulfur isotopes is inevitably more challenging experimentally; in this case, intermediate energy Coulomb-excitation of beams of radioactive nuclei produced in fragmentation reactions has been used in measurements of $B(E2; 0^+_{\text{g.s.}} \to 2^+)$, from which conclusions in relation to quadrupole collectivity can be made. Excitation energies and $B(E2; 0^+_{\text{g.s.}} \to 2^+)$ values for the lowest $J^\pi = 2^+$ states in neutron-rich ^{38,40,42}S from intermediate energy Coulomb-excitation measurements have provided the first evidence of moderate quadrupole deformation [$\beta = 0.31(9)$] at the major magic neutron number $N = 28$ [12,13]. The observed collectivity in ^{44}S can be reproduced with the relativistic mean field (RMF) calculations of Werner *et al.* [14], which predict large static quadrupole deformations for $^{40–44}$S. A similar collapse of the $N = 28$ shell closure has been observed in ^{42}Si [15]. Shape coexistence often becomes manifest in regions of shape change; in ^{44}S, evidence has been found of prolate-spherical shape coexistence [16]. In this case, the monopole strength of an 0^+_2 isomeric state at an excitation energy of 1365(1) keV is very small [$\rho^2(E0;\ 0^+_2 \to 0^+_1) = 8.7(7)\times10^{-3}$], which indicates a weak mixing between the prolate 0^+_1 ground state and the spherical 0^+_2 isomeric state. To date, ^{44}S is the heaviest sulfur isotope for which electromagnetic decay rates of excited states have been measured. For the moderately neutron-rich sulfur isotopes, such as those populated in the present work, the more detailed spectroscopic information available allows tests of state-of-the-art shell-model calculations and, in particular, the role of intruder states. One such example relates to the excitation energy of the yrast 6^+ state of ^{36}S. Shell-model calculations involving the *sd* shell predict an excitation energy of the state of 15.3 MeV, about 8.6 MeV above the experimentally observed value of 6.69 MeV [17], which is a strong indication of the importance the promotion of pairs of nucleons across the shell gap to form 2p-2h configurations. Indeed, shell-model calculations which include the fp shell are able to reproduce both the excitation energy of the yrast 6^+ state and the negative-parity yrast states [17]. For the stable and neutron deficient isotopes of sulfur, high spin states can more readily be populated using conventional fusion evaporation reactions. For example, states of ^{35}S have recently been studied to spin $(21/2\hbar)$ through the use of the ^{26}Mg(^{18}O, $2\alpha 1n$)^{35}S reaction; in this case the physics interest centered around a comparison of the experimental level scheme with that predicted in state-of-the-art large-scale shell-model calculations using the SDPF_ MSD4 interaction [18]. Similarly, high-spin states and lifetimes in ^{33}S have been studied using the ^{24}Mg(^{14}N, αp) reaction [19] and the results interpreted using shell-model calculations in the sd-fp space. On a completely different physics topic, the fundamental property of isospin symmetry of the nuclear interaction has been studied in the high-spin spectroscopy of the neutron-deficient ^{31}S nucleus and its mirror nucleus ^{31}P [20–22].

Here, we extend the study of the nuclear structure of a few of the previously studied $sdpf$-shell sulfur nuclei through the measurement of nuclear lifetimes and comparison is made with the results of state-of-the art shell-model calculations based on the PSDPF [23], SDPF-U [24], and FSU [25,26] effective interactions, also presented here. Shell-model calculations of the electromagnetic transition probabilities of excited states strongly depend on and are sensitive to the details of the wave functions of the two states involved in the transition. The assumed configuration space used in such calculations, the shell-model interaction, and the effective nucleon charges also have a direct effect on the calculated values. In the *sd* region, the neutron rich nuclei with $N \approx 20$ are spectacular examples of coexistence between spherical and deformed configurations and present excellent tests of the ability of state-of-the-art shell-model calculations to reproduce the experimental observables, namely excitation energies, J^π values, electromagnetic decay properties, and nuclear static moments.

Binary grazing and deep-inelastic reactions have been used extensively over the last few decades to study the structure of neutron-rich nuclei over a wide range of nuclear masses. The coupling of large solid-angle magnetic spectrometers to arrays of escape-suppressed Ge detectors in studies of this type (see, e.g., Refs. [27–30]) has represented a very significant experimental advance in relation to earlier techniques which exploited large arrays of escape-suppressed Ge γ-ray detectors but no particle identification (see, e.g., Refs. [31–33]).

In the present work, the relatively poor statistics have prevented lifetime measurements for the neutron rich sulfur isotopes studied previously. Lifetime measurements here have been possible for sulfur isotopes with mass numbers near that of the ^{36}S projectile. Since ^{36}S has a closed neutron shell, it is expected that the neighboring isotopes, differing from ^{36}S by a few neutrons, will be well described by the shell model, both in terms of the level structure and the electromagnetic decay properties of low-lying excited states.

The isotopes of sulfur for which lifetimes, or lifetime limits, have been established are ^{35}S, ^{36}S, ^{37}S, and ^{38}S with neutron numbers $N = 19$, 20, 21, and 22, respectively. Lifetime measurements from the same experiment for the isotopes of phosphorus with mass numbers $A = 33$, 34, 35, and 36 have been published [34], while those for the isotopes of Si with $A = 32$, 33, and 34 will be the subject of a future presentation [35].

II. EXPERIMENT

Yrast and near-yrast states of the final sulfur nuclei were populated using binary grazing reactions produced in the interaction of a 225-MeV (6 MeV/u) beam of $^{36}S^{9+}$ ions of average current 1 pnA, delivered by the Tandem-ALPI accelerator complex at the INFN Legnaro National Laboratory, Italy, with a thin ^{208}Pb target. The stretched Pb target of thickness 1 mg cm^{-2}, and isotopically enriched to 99.7% in ^{208}Pb, was deposited onto a 1 mg cm^{-2} Nb backing foil and mounted onto the Cologne differential plunger [1,2], with the niobium backing facing the incident beam. The beam energy at the center of the Pb target is 215 MeV, the same energy as that which was used in the earlier experiment, to which reference has been made above. The degrader foil, used in the differential plunger apparatus to reduce the velocity of projectile-like nuclei after they leave the Pb target, consisted of a 3 mg cm^{-2} Nb foil mounted at a short distance downstream from the target. The distance between the Pb target and degrader foil was adjusted and controlled by a piezoelectric feedback system developed at the University of Cologne [36]. As the recoiling projectile-like nucleus moves through the plunger towards the entrance to the PRISMA magnetic spectrometer, the probability of γ-ray emission before or after passage through the degrader foil depends on the distance between target and degrader foils, the effective lifetime of the decaying state, and the velocity of the emitting nucleus. If the lifetime is comparable to the flight time of the nucleus between the Pb target and degrader, two photopeak components are observed in the γ-ray energy spectrum for each γ-ray transition, corresponding to the different Doppler shifts associated with recoil velocities before and after passage through the degrader. The velocity vector of sulfur ions after passage through the degrader foil is determined from the reconstruction of their flight path through the PRISMA spectrometer (see later); the velocity before passage through the degrader foil was calculated from a knowledge of the energy loss in the degrader foil. For the exit channel corresponding to one proton transfer (^{35}P as the final nucleus), for example, the v/c values of the recoiling nucleus before and after passage through the degrader foil are 10.0% and 9.4%, respectively. With the present experimental setup, lifetime measurements from about 1 ps to about 100 ps are possible.

The plunger device was placed in the reaction chamber of PRISMA [3,4] with its axis at 14° with respect to the PRISMA optical axis. Projectile-like fragments, produced in binary grazing reactions, pass through the degrader foil and into the PRISMA magnetic spectrometer where they are detected and identified. PRISMA was positioned at 56° with respect to the beam axis, covering a range of angles including the grazing angle of the reaction. The PRISMA spectrometer consists of a quadrupole singlet and a dipole magnet separated by 60 cm. The (x, y) coordinates and time information of an ion entering the spectrometer are measured using a position-sensitive microchannel plate (MCP) detector [37] placed at 25 cm from the target. Following the passage of each ion through the magnetic elements, the coordinates of the trajectory and time information are measured again at the focal plane of the spectrometer using a ten-element 100-cm-long multiwire parallel-plate avalanche counter (MWPPAC) [38]. The position resolution of the MCP and MWPPAC is 1 mm in the horizontal (dispersive) direction and the time resolution of the MCP and MWPPAC combination is about 300 ps. Finally, the ions are stopped in a 10×4 element ionization chamber (IC) used for energy loss $\triangle E$ and total energy E measurements [37,38]. For each ion detected in PRISMA, the above measurements enable a determination of the atomic number Z, the mass number A, the ion charge state, and the time of flight, thereby allowing an unambiguous identification of each detected projectile-like nucleus. PRISMA has a solid angle of 80 msr, a momentum acceptance of ±10%, and a mass resolution of 1/300 via time-of-flight measurements. Reconstruction of the trajectory of each ion through the spectrometer together with the time-of-flight measurement was used to establish the velocity vector of each ion on an event-by-event basis, essential for lifetime measurements by the differential recoil-distance technique, which relies on an accurate knowledge of the velocity of the projectile-like nucleus and the distance between target and degrader foils.

The associated deexcitation γ rays emitted by the recoiling nuclei were detected by the AGATA Demonstrator array [39]. This new state-of-the-art germanium detector array was, at the time of the present experiment, composed of five triple cluster modules positioned at a distance of 18 cm from the reaction target and covering backward angles from 135° to 175°. The corresponding simulated full-absorption efficiency for γ rays of energy 1 MeV is about 7%. Digitized signal pulses from the 36-fold segmented germanium crystals were compared with a data base of simulated detector responses using a pulse-shape analysis algorithm [40] to determine the

loci of γ-ray interactions in the detector crystals. The resulting position resolution is better than 5 mm FWHM. The application of a γ-ray tracking algorithm [41] resulted in the energies of individual γ rays. Energies and interaction positions of γ rays were stored in list mode with a time stamp, which permitted a correlation to be established between γ-ray events and the associated projectile-like reaction products identified at the focal plane of PRISMA. To produce γ-ray spectra, a precise Doppler-shift correction was applied on an event-by-event basis using the measured recoil velocity vector after the degrader; this results in Gaussian-shape photopeaks unaffected by the velocity profile of the sulfur recoil ions. Doppler correction of γ-ray energies corresponding to decay between target and degrader is less precise and this leads to an increase in the width of the corresponding photopeak. To reduce the counting rate from ^{208}Pb x rays, a lead absorber of thickness 2 mm was placed between AGATA and the reaction chamber. In total, five different distances of 7, 20, 35, 65, and 120 μm between the target and the degrader foils of the Cologne differential plunger were used during the experiment. The experiment ran for 9 days, with between 1 and 2 days of data accumulated for each distance. The data-acquisition trigger was provided by timing signals from the large area multiwire parallel plate avalanche counter at the focal plane of PRISMA. Gamma-ray singles events were measured; the low statistics of the experiment prevented the accumulation of γ-γ coincidence data. A relative photopeak efficiency calibration for the AGATA array was carried out using radioactive sources of ^{152}Eu and ^{133}Ba. Uncertainties in γ-ray energies are approximately ± 1 keV.

In summary, lifetime measurements using the recoil-distance method have exploited the powerful combination of a large acceptance magnetic spectrometer, PRISMA, and a high efficiency γ-ray tracking array, AGATA, which results in good reaction channel selection and precise Doppler correction of γ-ray energy spectra.

III. RESULTS AND DISCUSSION

In the present experiment, a wide range of nuclear species, from Mg ($Z = 12$) to Ca ($Z = 20$), was identified at the focal plane of PRISMA. Here, we focus on a discussion of those isotopes of sulfur for which reaction yields were sufficiently large for the measurement of nuclear lifetimes to be made using the present experimental setup.

A. The isotopes of sulphur

The mass spectrum of Fig. 1 shows that the sulfur isotopes with mass numbers $35 \leqslant A \leqslant 38$ were successfully populated in the present work. As expected, the largest yield corresponds to ^{36}S as the final nucleus. The measured mass resolution is 1/140. A mass gate of suitable location and width was used to produce a one-dimensional γ-ray spectrum corresponding to the particular isotope of interest. Experimental results for the isotopes of sulfur for which lifetimes, or lifetime limits, have been established here will be presented together with the results of state-of-the-art shell-model calculations of the electromagnetic decay properties of the nuclear states

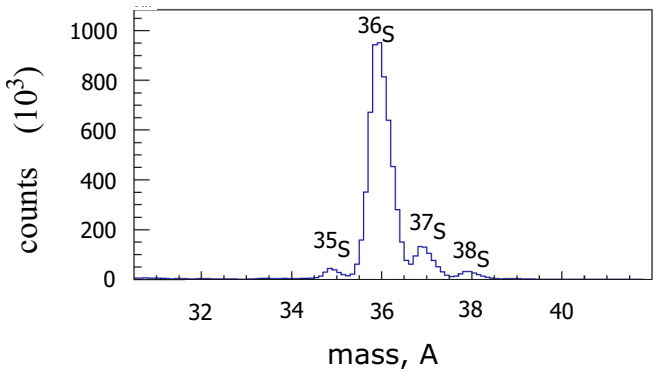

FIG. 1. Mass spectrum of the sulfur isotopes produced in the present work.

involved. Where previous lifetimes have been reported, they will be compared with the results of the present work. In those cases for which the accuracy of the published lifetime value is significantly better than that from the present experiment, the results of the current work, including the results of shell-model calculations, will nevertheless be presented in the interests of completeness.

The $(0+1)\hbar\omega$ states in the sulfur isotopes with $A = 35$ and 36 are described here with the PSDPF interaction [23]. This shell-model calculation has a ^{4}He core and uses the full *p-sd-pf* model space; it is built on existing interactions for the major shells with adjustments of the cross-shell parameters. The positive-parity states are essentially obtained using the USDB Hamiltonian, developed by Brown and Richter [42], which is included in the PSDPF interaction. Excitation of one nucleon is allowed across a major shell, from the *sd* shell to the *pf* shell in the present case. For the two-particle two-hole states of ^{36}S, and in particular the (6_1^+) state first identified by Liang *et al.* [17], the recently developed FSU interaction [25] has been used. For the isotopes of sulfur with $A = 37$ and 38, large scale $0\hbar\omega$ shell-model calculations were also performed using the NATHAN code [11,43,44] but with the SDPF-U effective interaction [24]. In this case, protons are restricted to the *sd* shell and neutrons are confined to the full *pf* shell-model space outside an inert ^{28}O core. In the calculation of $E2$ and $E3$ electromagnetic transition probabilities, effective charges of $e_{\rm eff}(p) = 1.36e$ and $e_{\rm eff}(n) = 0.45e$ were used while, for the calculation of $B(M1)$ and $B(M2)$ transition probabilities, the effective spin and orbital g factors of $g_{\nu s}^{\rm eff} = -3.55$, $g_{\nu \ell}^{\rm eff} = -0.09$, $g_{\pi s}^{\rm eff} = 5.150$, and $g_{\pi \ell}^{\rm eff} = 1.159$ were adopted [45].

B. Lifetimes in ^{35}S

^{36}S is a semimagic nucleus with a closed shell of 20 neutrons. Consequently, low-lying positive-parity states of ^{35}S with $J^\pi = 1/2^+$, $3/2^+$, and $5/2^+$ are expected to have wave functions with a large component corresponding to a neutron hole in the sd-shell. Unfortunately, direct single-neutron pickup reactions on ^{36}S have, to date, not been reported in the literature and thus the neutron single-hole characteristics of states of ^{35}S remain unexplored experimentally. The γ-ray spectrum measured in coincidence with ^{35}S ions detected and

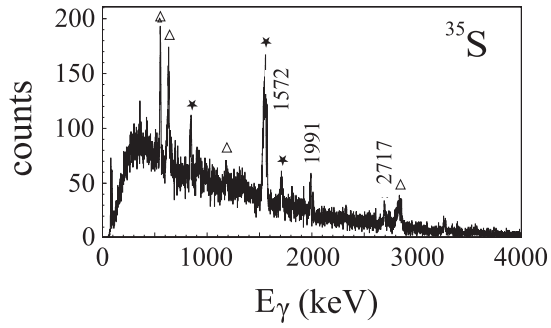

FIG. 2. Gamma-ray singles spectrum measured in coincidence with ^{35}S ions detected at the focal plane of the PRISMA spectrometer. The photopeaks labeled with a triangle and star correspond to γ rays from the associated target-like ^{208,209}Pb isotopes, respectively.

identified at the focal plane of the PRISMA spectrometer is shown in Fig. 2. All the labeled γ-ray peaks were identified in the previous experiment, carried out at the INFN Legnaro National Laboratory [10]. The level scheme from that study, which is consistent with that of the Nuclear Data Sheets evaluation [46], is shown in Fig. 3. In the more recent work of Aydin *et al.* [47], definite spin assignments of $7/2^+$, $9/2^-$, and $11/2^-$ have been made for the states at excitation energies of 3593, 3818, and 4023 keV, respectively. Dominating the γ-ray spectrum of Fig. 2 is the 1572-keV γ-ray photopeak, which corresponds to the deexcitation of the first excited $1/2^+$ state to the $3/2^+$ ground state.

The ground state of ^{35}S has a J^π value of $3/2^+$ and, in a simple single-particle shell-model picture, corresponds to a neutron hole in the $1d_{3/2}$ shell. The first-excited state at 1572 keV has a J^π value of $1/2^+$ and corresponds to a neutron hole in the $2s_{1/2}$ orbital, whereas the $5/2^+$ hole state is probably that at an excitation energy of 2717 keV. The known negative-parity states, such as that with $J^\pi = 7/2^-$ at an excitation energy of 1991 keV, probably correspond to one-particle two-hole states, in which the unpaired neutron populates the fp shell. In the present work, a measurement has been made of the lifetime of the $1/2^+$ first-excited state.

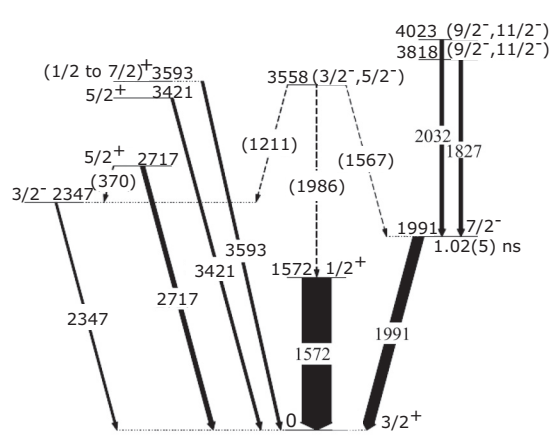

FIG. 3. The level scheme for ^{35}S observed in the earlier ^{36}S + ^{208}Pb experiment [10].

C. Lifetime of the $J^\pi = 1/2_1{}^+$ state of ^{35}S at 1572 keV

As discussed earlier, in a simple shell-model picture, the wave functions of the ground state and first excited $1/2^+$ state of ^{35}S are $\pi(1d_{5/2})^6(2s_{1/2})^2 \otimes \nu(1d_{5/2})^6(2s_{1/2})^2(1d_{3/2})^3$ and $\pi(1d_{5/2})^6(2s_{1/2})^2 \otimes \nu(1d_{5/2})^6(2s_{1/2})^1(1d_{3/2})^4$, respectively.

On this basis, the $1/2^+ \rightarrow 3/2^+$ transition is a mixed $M1$-$E2$ transition, where the $M1$ component is Δl "forbidden" [48] and corresponds to the transition $\nu(2s_{1/2}) \rightarrow \nu(1d_{3/2})$.

The lifetime of the $1/2^+$ state has previously been measured by Warburton *et al.* [49] in the early 1970s using the Doppler-shift attenuation method (DSAM); the nucleus of interest was formed using the ^{2}H(^{34}S, p)^{35}S reaction. The authors used three different target backing materials, Mg, Al, and Cu, as the stopping media for the ^{35}S γ-decaying nuclei. Three different lifetime values were obtained, namely 2.8(4) ps, 3.8(6) ps, and >3.0 ps, respectively, corresponding to the three different slowing-down media. The mean lifetime is 3.3(5) ps.

Note that, in the present case, the first-excited state is not fed significantly from the populated higher-lying states. For the lifetime measurements presented here, a "Q gate" is applied in order to minimize the effect of feeding of the states of interest from higher lying states, while preserving the direct feeding of the state. Unless conditions are applied to the experimental data, unobserved side-feeding transitions will also contribute to the measured lifetimes of the states discussed here. To minimize the effects of both direct and side-feeding, an energy condition was applied to the PRISMA focal-plane Q value, generated from the measurement of ejectile energy. The effect of changes to the upper and lower limits of the Q gate on the γ-ray intensity ratio (see below) used in the determination of the lifetime of the state was also investigated in order to confirm that, with an appropriate choice of gate, feeding of the state from higher lying states is negligible. The robustness of the method was validated by reproducing known lifetimes. If nondirect feeding of the states studied here were an issue, lifetime determinations would tend to be larger than the accepted values. As will be seen, this is certainly not the case. The lifetime comparisons presented later show that, of the five cases considered, four of the lifetime values based on the present analysis methods are indeed smaller than the accepted published values (although in agreement within experimental errors). This procedure will henceforth be referred to as corresponding to the application of a "Q gate."

In the present case, the incorrectly Doppler-shifted 1423-keV γ-ray transition ($15/2^- \rightarrow 9/2^+$) from the binary partner nucleus ^{209}Pb lies in this energy region of the γ-ray spectrum and this photopeak was also removed through the application of the Q gate. Figure 4 shows the Doppler corrected γ-ray spectrum with and without the ^{209}Pb contaminant γ-ray photopeak removed and Fig. 5 shows a section of the Doppler-corrected γ-ray spectra associated with the $1/2^+ \rightarrow 3/2^+$ transition in ^{35}S, at target-degrader distances of 20, 35, 65, and 120 μm. Gaussian fits for the two components of the photopeak are also presented, with appropriate background subtraction. The resultant decay curve corresponding to the $1/2^+ \rightarrow 3/2^+$ transition is given in Fig. 6; the measured

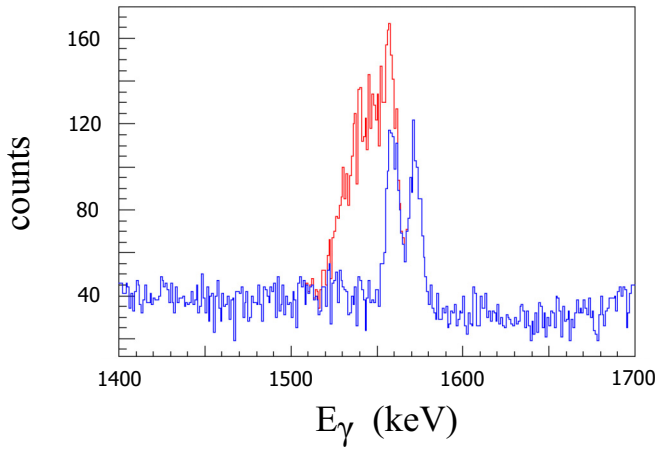

FIG. 4. A section of a measured ^{35}S γ-ray spectrum which shows the 1423-keV ^{209}Pb contaminant γ-ray photopeak (in red), and the same spectrum (in blue) with the photopeak removed through the application of a Q gate. This spectrum is a sum of spectra corresponding to all five target to degrader distances.

lifetime value is $\tau = 3.3(2)$ ps, which is in excellent agreement with the mean lifetime value obtained in the previous work of Warburton *et al.* [49] [3.3(5) ps], which is also the value quoted in the most recent Nuclear Data Sheets evaluation [46]. In Fig. 6, I_t is the intensity of γ rays emitted from recoiling ^{35}S nuclei during their passage from target to degrader, while I_d is the intensity of γ rays emitted after the recoiling nuclei have passed through the degrader foil. In this, and in all subsequent decay curves presented here, the natural logarithm of the ratio $I_d/(I_d + I_t)$ is shown as a

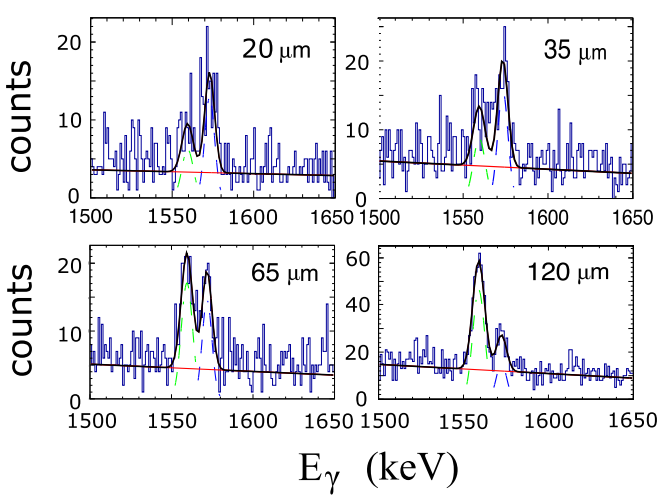

FIG. 5. Section of the measured γ-ray spectra for target-degrader distances of 20, 35, 65, and 120 μm, which shows the two components of the 1572-keV photopeak corresponding to the $1/2^+$ to $3/2^+$ (ground state) transition in ^{35}S. The black curve corresponds to a fit to the data (Gaussian peaks plus linear background). Background-subtracted photopeaks are shown in green (corresponding to γ-ray emission between the target and absorber) and in blue (corresponding to γ-ray emission after the decaying nucleus has passed through the degrader foil).

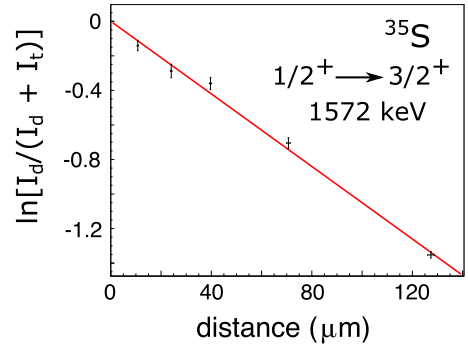

FIG. 6. The decay curve corresponding to the $1/2^+ \rightarrow 3/2^+$ transition in ^{35}S. See text for details.

function of the target to degrader distance. For all lifetime measurements here, and in other published lifetimes using the same experimental setup [29,34,50,51], the quoted error in the measured lifetime is dominated by the statistical uncertainty in the slope of the decay curve. Other contributions to the experimental uncertainty in lifetime are small by comparison; the precision of target-foil separation setting, with the piezoelectric feedback system used here, is around 0.1 μm [2], and the uncertainty in recoil velocity is less than 1% [39]. In a determination of the uncertainty in the lifetime, these uncertainties are combined with the statistical uncertainty in the slope of the measured decay curve. In the present and in earlier work using the same experimental setup [29,34], the areas of γ-ray photopeaks have been determined by fitting Gaussian shapes to the data; there is no evidence to suggest that this results in significant systematic errors in the determination of peak areas. Any small-percentage systematic error, to a good approximation the same for each peak, would have a very small effect on the γ-ray intensity ratios used in the determination of the decay curve. As noted above, the good agreement with previous independent lifetime measurements also confirms the robustness of the present method used in the determination of lifetimes. In particular, in addition to the above lifetime measurement of the $J^\pi = 1/2_1{}^+$ state of ^{35}S, excellent agreement has also been obtained in measurements of the lifetimes of the first excited 2_1^+ state of ^{34}P (1.5 ± 0.5 ps [34] compared with the previously accepted value of $1.9^{+0.9}_{-0.4}$ ps [52]) and of the $1/2^+$ state of ^{35}S at 1572 keV [3.3(2) ps compared with the adopted value of 3.3(5) ps [46]]. Similarly, the measured lifetime of the 3^- state of ^{36}S at 4193 keV, 0.84(24) ps, is in very good agreement with the most recent published value of 0.9(1) ps [53]. In addition, the measured lifetime of the first 2^+ state of ^{32}Si at an excitation energy of 4193 keV, namely 0.44(11) ps [35], is in excellent agreement with the measurement of Guillaume *et al.* [54], 0.48(7) ps. Thus, five lifetime measurements based on data from the same experiment are in excellent agreement with previously published values, and this provides strong validation of the analysis methods used here.

The shell-model excitation energy of the first excited $J^\pi = 1/2^+$ excited state is 1.739 MeV which agrees well with the experimental value of 1.572 MeV. The component in the wave function of the state with the configuration $\pi(1d_{5/2})^6(2s_{1/2})^2(1d_{3/2})^0 \otimes \nu(1d_{5/2})^6(2s_{1/2})^1$

$(1d_{3/2})^4$ corresponds to 44% of the total wave function. The other contributions of significance are $\pi(1d_{5/2})^6(2s_{1/2})^1(1d_{3/2})^1 \otimes \nu(1d_{5/2})^6(2s_{1/2})^2(1d_{3/2})^3$ (18%) and $\pi(1d_{5/2})^6(2s_{1/2})^0(1d_{3/2})^2 \otimes \nu(1d_{5/2})^6(2s_{1/2})^1(1d_{3/2})^4$ (14%). The $1/2^+$ state is therefore not such a pure hole state as the ground state, for which the wave-function component $\pi(1d_{5/2})^6(2s_{1/2})^2(1d_{3/2})^0 \otimes \nu(1d_{5/2})^6(2s_{1/2})^2(1d_{3/2})^3$ accounts for 77% of the total wave function. The shell-model value of lifetime, based on the PSDPF interaction, is 0.55 ps, which differs from the experimental value by a factor of about six.

The shell-model value of $B(E2;\ 1/2^+ \to 3/2^+)$ is 35.2 $e^2\,\mathrm{fm}^4$ (5.2 W.u.) while the $B(M1; 1/2^+ \to 3/2^+)$ value is 0.0204 μ_N^2 (1.14×10^{-2} W.u.). As noted earlier, the $B(M1)$ transition is Δl forbidden and this is reflected in the small shell-model value of $B(M1)$. The shell-model mixing ratio $[\delta^2 = \lambda(E2)/\lambda(M1)]$, for which there is currently no experimental measurement, is $|\,\delta\,| = 0.55$. However, it is noted here that the multipolarity of the 1572-keV transition has been assigned as $M1$ by Aydin *et al.* [47] on the basis of an angular distribution ratio measurement, although no mixing ratios were extracted for the observed transitions in ^{35}S.

Although the $M1$ transition is Δl forbidden, the total shell-model width of the $1/2^+$ state ($\Gamma = 1.21\times10^{-3}$ eV) is dominated by the $M1$ component of the electromagnetic transition, for which the partial width is 0.93×10^{-3} eV. It would therefore appear that the discrepancy between experimental and shell-model lifetimes can be attributed to problems in the calculation of $M1$ transition rates. A similar issue was noted in a recent publication on the lifetimes in the isotopes of phosphorus [34]. In that work, there is evidence that shell-model values of $M1$ transition rates for the $3/2_1^+ \to 1/2_1^+$ (ground state) and $5/2_1^+ \to 3/2_1^+$ transitions in ^{33}P underestimate the experimental values by a factor of between 5 and 10. The two-body matrix elements which involve both $1d_{5/2}$ and $1d_{3/2}$ orbitals are relatively poorly defined in the USDB interaction and this may contribute to the observed differences between experiment and shell model in the phosphorus case. Note that, in contrast with the ^{33}P case [34], here the shell-model value of $M1$ transition probability is large in relation to experimental observation. It is therefore also expected that the above shell-model value of mixing ratio will not be in agreement with the measured mixing ratio. In this respect, a measurement of the mixing ratio would provide useful additional information on the $M1$ transition rate. The ^{35}S ground-state quadrupole moment (Q) and nuclear magnetic-dipole moment have been measured. The shell-model values of $Q = 5.28\ e\,\mathrm{fm}^2$ and $\mu = 0.95$ nm are in very good agreement with the experimental values of $Q = 4.71(9)e\,\mathrm{fm}^2$ [55] and $\mu = +1.00(4)$ nm [56].

D. Lifetimes in ^{36}S

The γ-ray spectrum for ^{36}S is shown in Fig. 7. All of the γ-ray peaks have been observed and identified in the previous PRISMA-CLARA experiment [10]. Figure 8 shows the level scheme of ^{36}S from the earlier work [10]. The level scheme is in agreement with that of the 2012 Nuclear Data Sheets evaluation of Nica *et al.* [57], with the exception of the 1182-keV $(6^+) \to (4^+)$ transition observed by Wang [10,58].

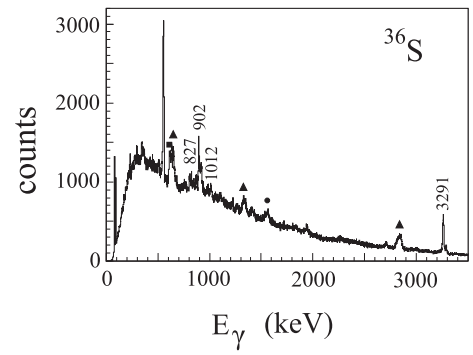

FIG. 7. Gamma-ray singles spectrum measured in coincidence with ^{36}S ions detected at the focal plane of the PRISMA spectrometer. The photopeaks labeled with a circle, square, and triangle correspond to γ rays from the associated target-like ^{206,207,208}Pb isotopes, respectively.

^{36}S is a stable nucleus with a closed shell of neutrons and four proton holes in the *sd* shell in its ground state. From a simple shell-model perspective, the ground state of ^{36}S, with $Z = 16$ and $N = 20$, has the configuration $\pi(1d_{5/2})^6(2s_{1/2})^2 \otimes \nu(1d_{5/2})^6(2s_{1/2})^2(1d_{3/2})^4$.

The significant energy gap between the $\pi(2s_{1/2})$ and $\pi(1d_{3/2})$ orbitals [59], together with a large $N = 20$ shell gap, leads to ^{36}S having characteristics of a doubly magic nucleus; the first excited 2^+ state is at an unusually high excitation energy of 3291 keV. Higher-lying positive-parity states involve the rearrangement of the eight *sd*-shell protons while negative-parity states involve neutron excitations into the *pf* shell.

^{36}S has been extensively studied experimentally, see Ref. [57] and references therein. Using the two-neutron transfer reaction, ^{34}S$(t,p\gamma)^{36}$S, Olness *et al.* [60] identified the first two excited states of ^{36}S at 3291 and 4193 keV, with

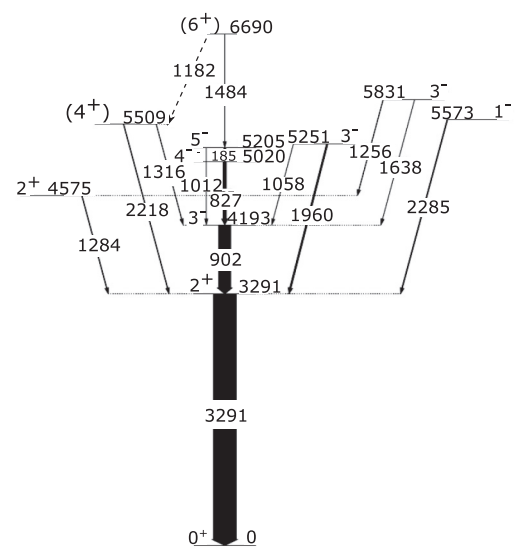

FIG. 8. The level scheme for ^{36}S observed in the earlier ^{36}S + ^{208}Pb experiment [10].

J^π assignments of 2^+ and 3^-, respectively. The levels at 5020 and 5205 keV were assigned J^π values of 4^- and 5^-, respectively, by Hogenbirk *et al.* [61]. A transition of energy 1484 keV was observed for the first time in a study by Liang *et al.* [17] and the γ-decaying state at 6690 keV was assigned a J^π value of (6^+). The first 2^+ state of ^{36}S at an excitation energy of 3291 keV is strongly populated in the present work, see Fig. 7. Its lifetime [110(30) fs] has been measured by Samworth and Olness, again using the ^{34}S$(t,p\gamma)^{36}$S reaction; a Doppler centroid shift method was used [62]. Using the Coulomb excitation of a ^{36}S beam in inverse kinematics, Speidel *et al.* [53] measured the lifetime [120(10) fs] using the Doppler-shift attenuation method. The g factor of the 2^+ state, $g = +1.3(5)$, was also determined for the first time using the transient field technique [53]. The evaluation of Nica *et al.* [57] gives the lifetime of the state as 120(10) fs. The lifetime is too short for a measurement with the present experimental setup. The 3291-keV photopeak is fully Doppler shifted in all γ-ray spectra in the present work, which is consistent with the measured lifetime. The corresponding experimental $B(E2; 2^+ \to 0^+)$ value is 17.6(15) e^2 fm^4 [2.49(21) W.u.], in reasonable agreement with the shell-model value of 3.14 W.u. The shell-model excitation energy (3335 keV) and lifetime (93 fs), based on calculations carried out as part of the present work using the PSDPF interaction, are in good agreement with experiment, as is the shell-model value of the g factor, +1.28. The calculation of g factor was made using the bare nucleon g factors. The dominant component (90%) in the wave function of the 2^+ state is $\pi(1d_{5/2})^6(2s_{1/2})^1(1d_{3/2})^1 \otimes \nu(1d_{5/2})^6(2s_{1/2})^2(1d_{3/2})^4$.

In the present work, lifetimes have been measured for the first $J^\pi = 3^-$ state and the first (6^+) state.

E. Lifetime of the $J^\pi = 3_1^-$ state of ^{36}S at 4193 keV

In the measurement of the lifetime of the 3_1^- state, it is necessary to consider the direct feeding contributions from the 4^- (827-keV transition), 5^- (1012-keV transition), and 3_2^- (1058-keV transition) states in addition to the unobserved side feeding. In relation to the intensity of the 902-keV $3_1^- \to 2_1^+$ transition, the γ-ray intensities of the 827-, 1012-, and 1058-keV transitions are 28.0(8)%, 2.6(5)%, and 1.9(5)%, respectively. Figure 9 shows a section of the γ-ray energy spectrum with and without the setting of a Q gate. The spectrum in blue corresponds to no Q-gate condition; the feeding transitions at energies of 827 and 1012 keV can be seen together with the two components of the photopeak corresponding to the 902-keV transition. The γ-ray energy spectrum in red corresponds to the application of a Q-gate condition; it may be seen that the feeding transitions are reduced in intensity in relation to the photopeak of interest. As noted earlier, in this and in other cases of lifetime measurements where a Q-gate condition was applied, it was checked that the γ-ray intensity ratio, $I_d/(I_d + I_t)$, does not exhibit any significant dependence on the detailed choice of limits for the Q gate.

Figure 10 presents a section of the measured γ-ray spectra for target-degrader distances of 7, 20, 35, and 120 μm and shows the 902-keV photopeak corresponding to the transition $3_1^- \to 2_1^+$; Gaussian fits with a linear background subtraction are shown for the two components of the photopeak. The

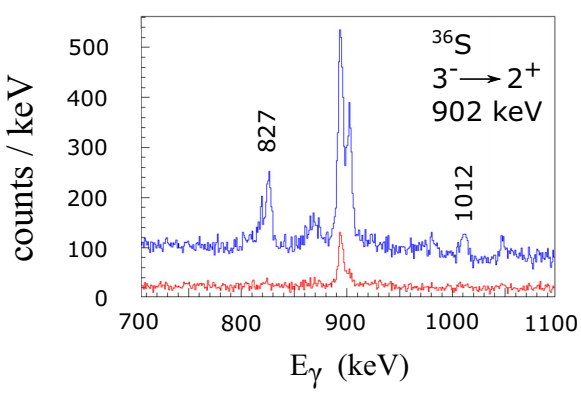

FIG. 9. Section of the ^{36}S γ-ray energy spectrum with and without Q conditions set to remove feeding from higher-lying states and from unobserved side-feeding states.

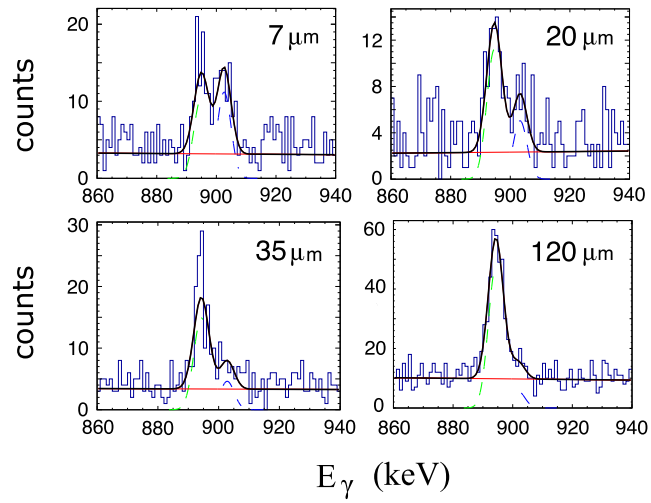

FIG. 10. Section of the measured γ-ray spectra for target-degrader distances of 7, 20, 35, and 120 μm which shows the two components of the photopeak corresponding to the 902-keV $3_1^- \to 2_1^+$ transition in ^{36}S. See also caption to Fig. 5.

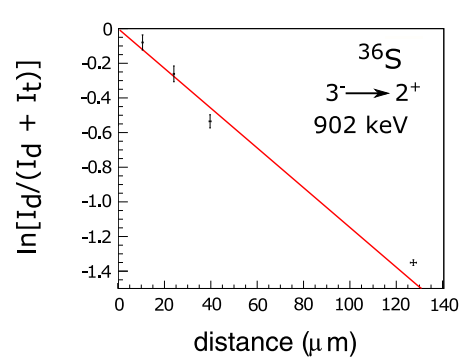

FIG. 11. Decay curve for the ^{36}S $3_1^- \to 2_1^+$ transition. See text for details.

TABLE I. Experimental and shell-model values of excitation energies and lifetimes of states in ^{36}S. Adopted lifetimes for the 2^+ and 3_1^- states are from the Nuclear Data Sheets evaluation of Nica *et al.* [57] and are based on the measurements of Speidel *et al.* [53]. See text for details.

J^π	E (expt.) (keV)	E (SM) (keV)	τ (present) ps	τ (adopted) ps	τ (SM) ps
2^+	3291	3335	<1	0.12(1)	0.093
3_1^-	4193	4293	0.84(24)	0.9(1)	0.25
(6^+)	6690	7188	5.4(26)		4.3

corresponding decay curve is presented in Fig. 11; the resultant lifetime is $\tau = 0.84(24)$ ps.

Speidel *et al.* [53] have made the most recent published measurement of the lifetime of the 3_1^- state (0.9(1) ps) using the Doppler-shift attenuation method in the inverse kinematics Coulomb excitation of ^{36}S; this value is in excellent agreement with that from the present work [0.84(24) ps]. The results of shell-model calculations based on the PSDPF interaction reproduce the energy of the 4193-keV 3_1^- state very well (4293 keV); the shell-model lifetime of 0.25 ps is not in particularly good agreement with experiment but is nevertheless of the same order of magnitude as the experimental value. Table I presents a summary of the experimental and shell-model energies and lifetimes of the three states of interest here, namely, the first 2^+ state, the first 3_1^- state, and the yrast (6^+) state of ^{36}S, and Table II presents the experimental and shell-model values of the electromagnetic decay properties of the three states of interest in ^{36}S.

The shell-model wave function of the 3_1^- state has two main components. These correspond to the configurations $\pi(1d_{5/2})^6(2s_{1/2})^2(1d_{3/2})^0(1f_{7/2})^0 \otimes \nu(1d_{5/2})^6(2s_{1/2})^2(1d_{3/2})^3(1f_{7/2})^1$ (31%) and $\pi(1d_{5/2})^6(2s_{1/2})^1(1d_{3/2})^0(1f_{7/2})^1 \otimes \nu(1d_{5/2})^6(2s_{1/2})^2(1d_{3/2})^4(1f_{7/2})^0$ (19%). The 3_1^- state decays to the 2_1^+ state by an $E1$ or $M2$ transition; the shell model reduced transition probabilities are $B(E1) = 0.0034\ e^2\,\mathrm{fm}^2$ (0.0049 W.u.) and $B(M2) = 6.6\mu_N^2\ \mathrm{fm}^2$ (0.37 W.u.). The shell-model mixing ratio $[\delta^2 = \lambda(M2)/\lambda(E1)]$ is $|\delta| = 3.7\ 10^{-3}$; the transition is therefore, as expected, dominated by $E1$ radiation. An experimental mixing ratio $[\delta = +0.03(3)]$ has been measured by Olness *et al.* [60] (see also Ref. [57]) using the ^{34}S$(t, p\gamma)$ two-neutron transfer reaction, in agreement with the shell-model value; the transition is therefore essentially pure $E1$ in nature. The corresponding experimental $B(E1; 3^- \to 2^+)$ value is 0.00135(15) W.u. [57]. It is noted here that shell-model values of $B(E1)$ using the PSDPF interaction are normally small compared with experimental values [63]; this is not the case here for the decay of the 3_1^- state.

The decay branch to the 0^+ ground state by an $E3$ transition has not been observed experimentally. The shell-model branching ratio is $I_\gamma(3_1^- \to 0^+)/I_\gamma(3_1^- \to 2_1^+) = 0.0041$, and this is consistent with the nonobservation of the $3_1^- \to 0^+$ transition in this or in earlier work; see Ref. [57] and references therein. It is noted here that the shell-model value of $B(E3;3_1^- \to 0^+)$ is large, namely, 77.0 $e^2\,\mathrm{fm}^6$ (15.9 W.u.) and this is consistent with an $E3$ transition corresponding to the unpaired proton making the $\Delta j = \Delta\ell = 3$ transition $\pi(1f_{7/2}) \to \pi(2s_{1/2})$.

F. Lifetime of the $J^\pi = (6_1^+)$ excited state of ^{36}S at 6690 keV

The 1484-keV γ-ray photopeak, corresponding to the $(6_1^+) \to 5_1^-$ transition, has two components in the ^{36}S γ-ray spectrum. Although there is no observed feeding to this state from higher-lying states, a Q gate has nevertheless been employed in order to produce γ-ray spectra which correspond to a more selective population of the (6_1^+) state. Figure 12 presents a section of the measured γ-ray spectra for target-degrader distances of 7, 35, and 120 μm. The statistics for the γ-ray photopeak corresponding to the $(6_1^+) \to 5_1^-$ transition are very poor; nonetheless, a clear evolution of the relative intensities of the two components of the photopeak can be seen with changing target-degrader distance. Figure 13 presents the decay curve for the (6_1^+) state; the resultant lifetime of $\tau = 5.4(26)$ ps has a large associated statistical error. The value of lifetime based on the 120 μm data, with the

TABLE II. Experimental and shell-model values of electromagnetic decay properties of states in ^{36}S. The experimental $B(E2;2^+ \to 0^+)$ value is based on the measurement of lifetime by Speidel *et al.* [53]. The mixing ratio for the $3_1^- \to 2^+$ transition is based on the work of Olness *et al.* [60]. The $B(E1;3_1^- \to 2^+)$ value has been taken from Ref. [57] and is based on the lifetime measurement of Speidel *et al.* [53]. The branching ratio of the (6^+) state is from Refs. [10,58]. All other electromagnetic transition probabilities for the (6^+) state are from the present work.

J^π	E (keV)	E_f, J_f^π (keV)	BR (expt.) (%)	BR (SM) (%)	δ (expt.)	$\lvert\delta\rvert$ (SM)	$B(E1)$ (expt.) (W.u.)	$B(E1)$ (SM) (W.u.)	$B(E2)$ (expt.) (W.u.)	$B(E2)$ (SM) (W.u.)	$B(M2)$ (SM) (W.u.)
2^+	3291	$0, 0^+$	100	100					2.49(21)	3.14	
3_1^-	4193	$0, 0^+$	0	0.4							
		$3291, 2^+$	100	99.6	+0.03(3)	$3.7\ 10^{-3}$	0.00135(15)	0.0049			0.37
(6^+)	6690	$5205, 5^-$	35(7)	19			$1.78(90)\ 10^{-5}$	$1.20\ 10^{-5}$			
		$5509, (4^+)$	65(13)	81					6.0(36)	9.4	

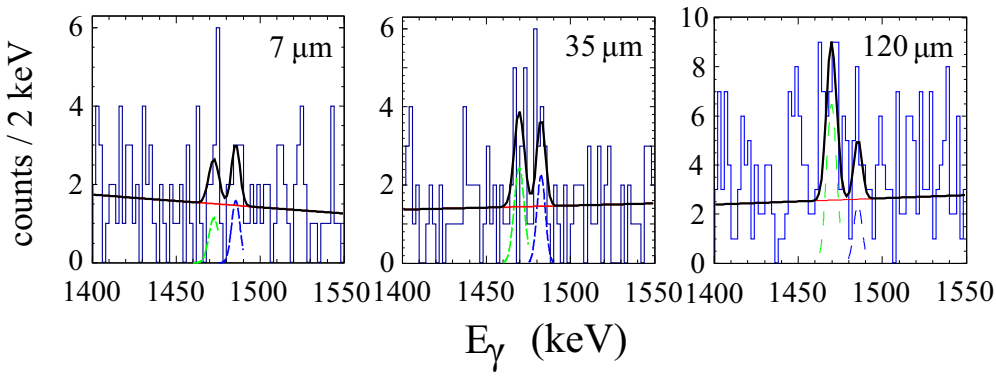

FIG. 12. Section of the measured γ-ray spectra for target-degrader distances of 7, 35, and 120 μm which shows the two components of the 1484-keV photopeak corresponding to the $(6_1^+) \rightarrow 5_1^-$ transition in ^{36}S.

photopeak areas measured by integration with linear background subtraction, is 5.1(30) ps; this provides additional confidence in the value of the lifetime given here.

To make a comparison between experiment and shell model for the properties of the 6_1^+ state, it is necessary to include configurations which correspond to the promotion of two nucleons across the shell gap into the pf shell, since the wave function of the state has very significant two particle-two hole components in its wave function. However, the PSDPF interaction allows the promotion of only one nucleon from the sd-shell into the fp shell. Thus, the Strasbourg shell-model code based on the PSDPF interaction is unable to perform the necessary calculation of excitation energy and electromagnetic decay properties for the 6^+ state of ^{36}S.

Using the recently developed FSU interaction [25,26], the spectrum of 6^+ states of ^{36}S with both 0p-0h and 2p-2h configurations has been calculated with an ^{16}O core. The calculated states are unmixed, since no fits were made to 0p-0h or 2p-2h states to develop the interaction. Therefore, for the 2p-2h states, the valence space is $sdfp$; two particles are promoted from the sd to the fp shell. Excitation energies and orbit occupations for the 0p-0h and 2p-2h yrast 6^+ state are presented in Table III. The very significant discrepancy between the experimental excitation energy of 6.090 MeV and the excitation energy corresponding to the 0p-0h shell-model calculation serves to emphasize the crucial role played by the occupation of the fp shell in the structure of the 6_1^+ state.

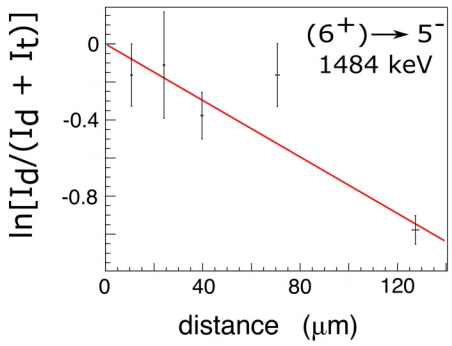

FIG. 13. The decay curve corresponding to the $(6^+) \rightarrow 5_1^-$ transition in ^{36}S. See text for details.

The shell-model calculation based on a 2p-2h configuration is able to reproduce the experimental excitation energy very well (7.188 MeV compared with 6.690 MeV). From Table III it may be seen that, in the 6^+ state, two neutrons occupy the $1f_{7/2}$ orbital to a good approximation and that there is a redistribution of protons within the sd shell, with a very insignificant occupation of the fp shell.

In the earlier experiment carried out at the INFN Legnaro Laboratory, to which reference was made above, a γ-ray photopeak of energy 1182 keV was identified [10,58] in the γ-ray spectrum corresponding to the identification of ^{36}S ions at the focal plane of PRISMA. The tentative placement to the $(6^+) \rightarrow (4^+)$ transition (see Fig. 8) was based solely on energy considerations. The 1182-keV photopeak is not observed in the present work. In the earlier work [10,58], the quality of the γ-ray spectrum near 1200 keV, where there are several close-lying photopeaks, is considerably better than is the case here. From the measured lifetime of the (6^+) state, $\tau = 5.4(26)$ ps, and the measured branching ratio, $I_\gamma((6^+) \rightarrow (4^+))/I_\gamma((6^+) \rightarrow 5^-) = 1.84(55)$ [10,58], it is possible to calculate the electromagnetic decay properties of the (6^+) state, which, it is assumed, decays to the (4^+) state by a pure $E2$ transition and to the 5^- state by a pure $E1$ transition. The resulting values are $B(E1; (6^+) \rightarrow 5^-) = 1.25(65)\times10^{-5}$ $e^2\,\mathrm{fm}^2$ $[1.78(90)\times10^{-5}$ W.u.] and $B(E2; (6^+) \rightarrow (4^+)) = 42(25)$ $e^2\,\mathrm{fm}^4$ [6.0(36) W.u.]. The electromagnetic decay properties of the 6^+ state were also calculated. As has been noted in the earlier work on the isotopes of phosphorus [34], the calculation of $E1$ transition rates in this region of the nuclear chart presents challenges. The shell-model values are $B(E1; 6^+ \rightarrow 5^-) = 0.84\times10^{-5}$ $e^2\,\mathrm{fm}^2$ $(1.20\times10^{-5}$ W.u.) and $B(E2; 6^+ \rightarrow 4^+) = 67$ $e^2\,\mathrm{fm}^4$ (9.43 W.u.). The corresponding lifetime of the 6^+ state is 4.3 ps, which agrees reasonably well with the experimental value of 5.4(26) ps, see Table I. Note that, in the shell-model calculations, the lifetime of the 6^+ state depends mainly on the $E2$ transition probability. The shell-model value of branching ratio, $I_\gamma(6^+ \rightarrow 4^+)/I_\gamma(6^+ \rightarrow 5^-) = 4.30$, is in poor agreement with the experimental value, 1.84(55), see Table II. Here, it is again worth emphasizing that the current proposed decay modes of the (6^+) state require to be confirmed by further measurement.

TABLE III. Shell-model values of excitation energy and orbit occupations for the yrast 6^+ state of ^{36}S. The FSU interaction was used in the calculations.

	0p-0h calculation			2p-2h calculation		
Orbit	Excitation energy (MeV)	Neutron occupation	Proton occupation	Excitation energy (MeV)	Neutron occupation	Proton occupation
$1d_{5/2}$	16.085	6.00	3.98	7.188	5.78	5.51
$1d_{3/2}$		4.00	2.02		2.62	1.18
$2s_{1/2}$		2.00	2.00		1.63	1.29
$1f_{7/2}$		0.00	0.00		1.82	0.02
$1f_{5/2}$		0.00	0.00		0.06	0.00
$1p_{3/2}$		0.00	0.00		0.10	0.00
$1p_{1/2}$		0.00	0.00		0.00	0.00

Finally, it is noted that, based on the average strength of the $E1$ isovector transition in the $A = 36$ mass region [64], Liang *et al.* [17] proposed that the (6_1^+) state would have a lifetime of 1.1 ps; the measured lifetime is of the same order of magnitude.

G. Lifetimes in ^{37}S

In the present work, lifetime limits have been established for two states in ^{37}S, namely, the first-excited state at 646 keV with $J^\pi = 3/2^-$ and the $(11/2_1^-)$ state at 2776 keV. These two states were strongly populated in the earlier work of Chapman *et al.* [6] which, as previously noted, used the same beam and target combination.

From the simplest perspective of the nuclear shell model, the $^{37}_{16}$S$_{21}$ ground state has four proton holes in the *sd* shell and one neutron in the $1f_{7/2}$ orbital outside the $N = 20$ shell closure and has a J^π value of $7/2^-$. Excited states of ^{37}S correspond to the rearrangement of protons within the *sd* shell and to promotion of the odd-neutron across the $N = 28$ shell gap to the higher-lying $2p_{3/2}$, $2p_{1/2}$, and $1f_{5/2}$ shell-model orbitals. In addition, the coupling of the odd $1f_{7/2}$ neutron to states of the ^{36}S core gives rise to multiplets of states. The lowest-lying core state of ^{36}S, the first $J^\pi = 2^+$ state, lies at an excitation energy of 3291 keV; consequently, core-excited states of ^{37}S are expected to be observed at around this energy, with J^π values of $3/2^-$, $5/2^-$, $7/2^-$, $9/2^-$, and $11/2^-$. ^{37}S is thus a good nucleus within which to study *n-p* cross-shell interactions and single-particle states around the $N = 20$ shell closure.

The first-excited state of ^{37}S at 646 keV was identified by Ajzenberg-Selove and Igo [65] using the ^{37}Cl$(t, {}^3$He$)^{37}$S charge-exchange reaction. This state was assigned a J^π value of $3/2^-$ by Thorn *et al.* [66] from proton angular distribution measurements in the ^{36}S$(d, p)^{37}$S one-neutron transfer reaction, in which states with excitation energy up to 5.72 MeV ($J^\pi = 5/2^-$) were observed; spectroscopic factors were measured for most states. In the ^{36}S$(d, p)^{37}$S reaction [66], the ground state is populated in $l = 3$ neutron transfer with a spectroscopic strength of $(2j + 1)S = 6.2$ and this is consistent, within the normal uncertainties associated with a distorted-wave Born approximation (DWBA) analysis, with a description of the ^{37}S ground state in terms of a ^{36}S ground-state core and the unpaired neutron occupying the $1f_{7/2}$ orbital outside the core. Similarly, most of the $2p_{3/2}$ neutron-transfer strength, $(2j + 1)S = 2.6$, is located in the 646-keV $J^\pi = 3/2^-$ first-excited state. The results of shell-model calculations [6] indicate that about 20% of the wave function of the first excited $J^\pi = 3/2^-$ state corresponds to the coupling of a $1f_{7/2}$ neutron to the first excited $J^\pi = 2^+$ state of the ^{36}S core, and this component cannot, of course, be populated in a direct one-neutron transfer process. The relatively strong population of the non-yrast 646-keV $J^\pi = 3/2^-$ first-excited state in the present work is consistent with single-neutron transfer playing an important role.

The strong 2776-keV transition has previously been assigned to the decay of the 2776-keV excited state to the ground state [6]. There is no previous credible evidence for its population in a direct single-neutron transfer reaction and its strong population here suggests that it is yrast; a tentative J^π value of $(11/2_1^-)$ has been assigned, based on the population characteristics of binary grazing reactions and on comparison with the results of shell-model calculations [6]. With this proposed assignment, decay to the ground state takes place through an $E2$ transition. The shell-model $11/2^-$ yrast state lies at an excitation energy of 2678 keV, in reasonably good agreement with the experimental value of the proposed $(11/2_1^-)$ state at 2776 keV. The wave function of the state is dominated (76%) by the configuration $\pi(1d_{5/2})^6(2s_{1/2})^1(1d_{3/2})^1 \otimes \nu(1d_{5/2})^6(2s_{1/2})^2(1d_{3/2})^4(1f_{7/2})^1$.

In this configuration, protons coupled to a J^π value of 2^+ are aligned with the total angular momentum of the odd $1f_{7/2}$ neutron. Of course, there is more than one core configuration with an angular momentum of 2^+. For example, the first 2^+ state of ^{36}S has, as the dominant configuration (90%), $\pi(1d_{5/2})^6(2s_{1/2})^1(1d_{3/2})^1 \otimes \nu(1d_{5/2})^6(2s_{1/2})^2(1d_{3/2})^4$, while the dominant configuration (93%) of the second 2^+ state, at a measured excitation energy of 4575 keV, is $\pi(1d_{5/2})^6(2s_{1/2})^0(1d_{3/2})^2 \otimes \nu(1d_{5/2})^6(2s_{1/2})^2(1d_{3/2})^4$. It would therefore seem reasonable to describe the $11/2^-$ state in terms of an unpaired neutron in the $1f_{7/2}$ orbital coupled to the first 2^+ state of the ^{36}S core.

The state at 2776 keV has previously been populated in the ^{37}Cl$(t, {}^3$He$)^{37}$S charge-exchange transfer reaction [65]; it would seem likely that population occurs through the pickup of a $2s_{1/2}$ proton from the ^{37}Cl ground state and the transfer of a neutron to the empty $1f_{7/2}$ shell. The observed population in

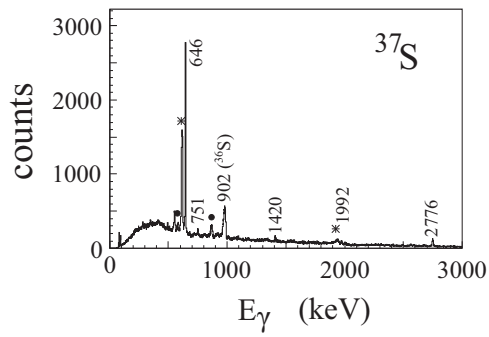

FIG. 14. Gamma-ray singles energy spectrum observed in coincidence with ^{37}S ions detected at the focal plane of the PRISMA spectrometer. The photopeaks labeled with a circle and asterisk correspond to γ rays from the associated target-like ^{206,207}Pb isotopes, respectively.

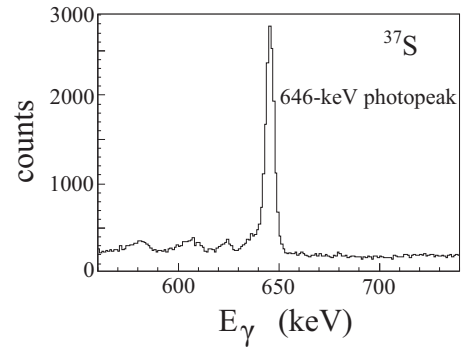

FIG. 16. A section of the ^{37}S γ-ray spectrum showing the 646-keV γ-ray photopeak. The spectrum corresponds to a sum of spectra measured at all target-degrader distances. Only one component of the photopeak is observed: that corresponding to γ-ray emission after the degrader foil.

the $(t, {}^3\text{He})$ reaction provides additional evidence in support of the proposed assignment.

The γ-ray spectrum measured in coincidence with ^{37}S ions detected and identified at the focal plane of the PRISMA spectrometer is shown in Fig. 14. All the labeled γ-ray peaks were identified in the previous experiment, referred to above [6]. The spectrum is dominated by γ rays corresponding to the decay of the first-excited state at 646 keV. The 2776-keV photopeak, corresponding to the transition from the $(11/2_1^-)$ excited state at 2776 keV to the ground state can also be seen. The level scheme from the previous study [6] is shown in Fig. 15.

H. Lifetime of the $J^\pi = 3/2^-$ 646-keV first-excited state of ^{37}S

For the $3/2^- \to 7/2_1^-$ transition, only the component corresponding to γ-ray emission after passage of the excited recoiling ^{37}S ions through the degrader foil is seen in the γ-ray spectrum of Fig. 16, which corresponds to the sum of all spectra measured at the five target to degrader distances. It can therefore be concluded that the lifetime of the $3/2^-$ state exceeds the maximum lifetime range corresponding to the present plunger setup, namely in excess of 100 ps. Figure 17 presents a graph of the calculated percentage of γ rays emitted from recoils before passage through the degrader foil as a function of target to degrader distance for lifetimes in the range from 1 to 100 ps. The longest lifetime that can be measured with the current setup is around 100 ps. The lifetime of the $3/2_1^-$ state has recently been measured by Wang *et al.* [67] using a β-γ delayed coincidence technique. The current lifetime limit of $\tau > 100$ ps is consistent with the published value of 193(14) ps. Shell-model calculations based on the SDPF-U interaction give a lifetime of 180 ps for the $3/2^-$ state, in excellent agreement with the experimental value. The shell-model value of $B(E2; 3/2^- \to 7/2^-)$, namely, 20.0 e^2 fm^4 (5.38 W.u.), is also in excellent agreement with the experimental value of 18.8(4) e^2 fm^4 [5.13(11) W.u.] [67], of course. Thus, a $0\hbar\omega$ sd-pf shell-model calculation in which the full sd (pf) valence space was used for protons (neutrons) above an ^{16}O core is very successful in its description of the first $3/2^-$ state of ^{37}S and its electromagnetic decay properties. It follows that the suggested mixing [67] of the $7/2^-$ ground state and the $3/2^-$ first-excited state with intruder $3/2^-$ and $7/2^-$ states at excitation energies of 1992 and 2023 keV, respectively, (which are not described within the configuration space of the present shell-model calculation [6]) is not

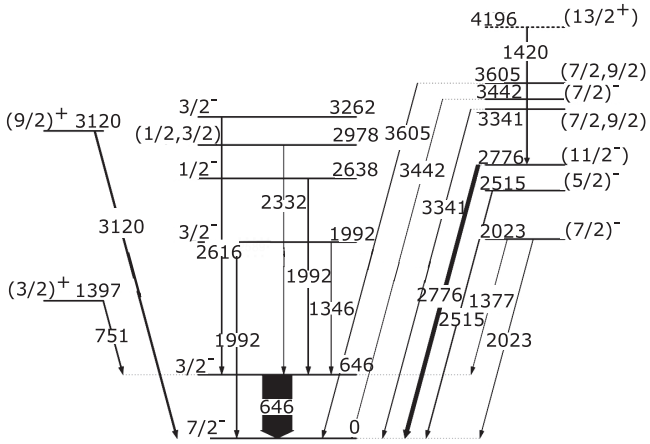

FIG. 15. The level scheme for ^{37}S based on the earlier ^{36}S + ^{208}Pb experiment [6].

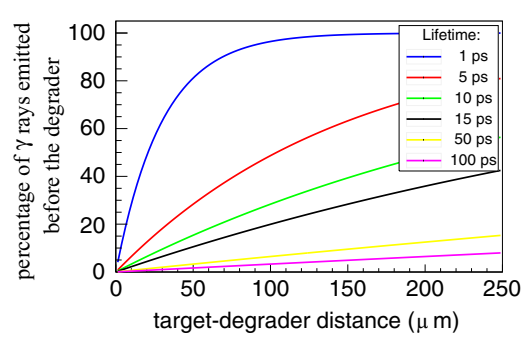

FIG. 17. Results of the calculation of the percent of γ rays emitted before passage through the degrader foil for target-degrader distances up to 250 μm. Calculations have been performed for lifetimes in the range from 1 to 100 ps.

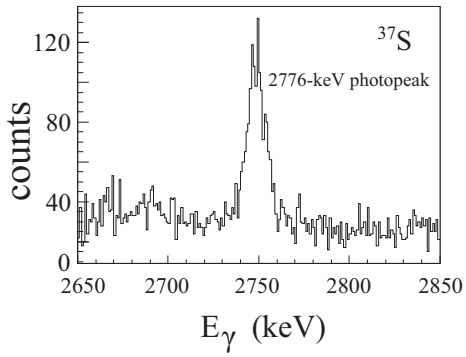

FIG. 18. Section of a γ-ray spectrum for ^{37}S which shows the 2776-keV photopeak and corresponding to a sum of all spectra measured at the five different target-to-degrader distances.

necessary for a good shell-model description of the excitation energy (624 keV) and, in particular, the electromagnetic decay properties of the first $3/2^-$ state.

I. Lifetime of the $J^\pi = (11/2^-)$ state of ^{37}S at 2776 keV

For the 2776-keV γ-ray photopeak, corresponding to the $(11/2^-) \rightarrow 7/2^-$ (ground state) transition, only the component corresponding to γ rays emitted before the degrader is observed, see Fig. 18. The figure corresponds to a sum of all spectra measured at the five target to degrader distances. On this basis, the lifetime of the state is estimated as <1 ps. Shell-model calculations, based on the SDPF-U interaction, give a lifetime of $\tau = 0.15$ ps, consistent with the measured experimental limit, and a $B(E2; 11/2^- \rightarrow 7/2^-)$ value of 33.0 e^2 fm^4 (4.5 Wu). In relation to the earlier discussion of the shell-model configuration of the $11/2^-$ state, it is noted here that the measured lifetime of the 2^+ core state of ^{36}S is 120(10) fs [53,57], and this is consistent with the present lifetime limit of the $(11/2^-)$ state. The corresponding shell-model lifetime values are 93 fs for the 2^+ state and 150 fs for the $11/2^-$ state.

J. Lifetimes in ^{38}S

The ground state of ^{38}S has, in a simple shell-model picture, two neutrons occupying the $1f_{7/2}$ orbital, outside an inert ^{36}S core. Figure 19 presents the decay scheme of ^{38}S, based on the earlier PRISMA-CLARA experiment [10] and Fig. 20 shows the γ-ray spectrum measured in the present work and corresponding to a sum of spectra measured at all target-degrader distances. The spectrum is dominated by the 1292-, 1534-, and 849-keV photopeaks corresponding to the deexcitation of the yrast 2^+, 4^+, and (6^+) states, respectively. Here, a limit will be established for the lifetime of the (6^+_1) state.

An evaluation of the literature for $A = 38$ nuclides has recently been published by Chen [68]. In relation to the yrast states with $J^\pi = 2^+$, 4^+, and (6^+) observed in the present work, there is agreement with earlier published studies of ^{38}S [8,32]. While the energy of the $(6^+) \rightarrow 4^+$ transition from the present work [849(1) keV] and the work of Wang *et al.* [8] is in agreement with that of Fornal *et al.* [32] (849

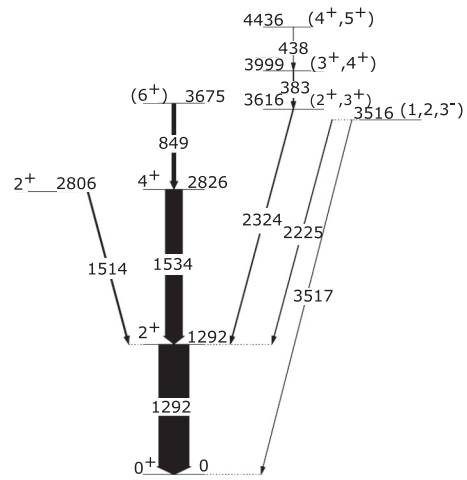

FIG. 19. A partial level scheme for ^{38}S based on the earlier ^{36}S + ^{208}Pb experiment [10,58].

keV), it is in disagreement, within experimental errors, with that quoted by Lunderberg *et al.* [69] [833(5) keV]. However, the position and shape of the 833-keV photopeak in the work of Lunderberg *et al.* is consistent with the emission of a 849-keV γ ray from a state that has a mean lifetime τ between 100 and 200 ps. Nevertheless, the evaluation of Chen [68] places the yrast (6^+) state at an excitation energy of 3658(6) keV, based on the 833-keV photopeak; the available evidence strongly suggests that this is incorrect. A state at excitation energy 3690(17) keV was observed in the ^{36}S(t, p) ^{38}S two-neutron transfer reaction [70] with an orbital angular-momentum transfer of $L = 5$ or 6 ($J^\pi = 5^-$ or 6^+), and this is also consistent with the proposed 6^+ spin and parity assignment. In relation to the non-yrast states observed in the earlier PRISMA-CLARA experiment [10], the 3516- and 4436-keV states are included in the evaluation of Chen [68] with J^π values of $(1, 2^+)$ and (4^+) respectively; the 3616- and 3999-keV states have not, on the other hand, been reported in the literature. The γ-ray transitions of energy 383 and 438 keV are included in the evaluation of Chen [68], but unplaced.

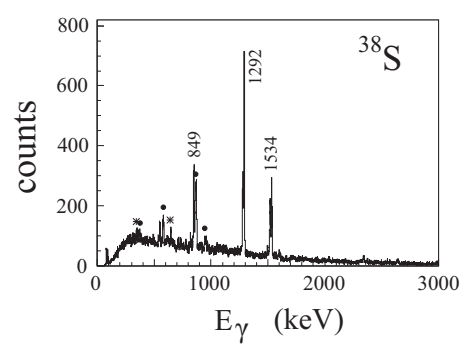

FIG. 20. Gamma-ray singles spectrum measured in coincidence with ^{38}S ions detected at the focal plane of the PRISMA spectrometer. The photopeaks labeled with an asterisk and a circle correspond to γ rays from the associated target-like nuclei, namely, ^{206}Pb and ^{207}Pb isotopes, respectively.

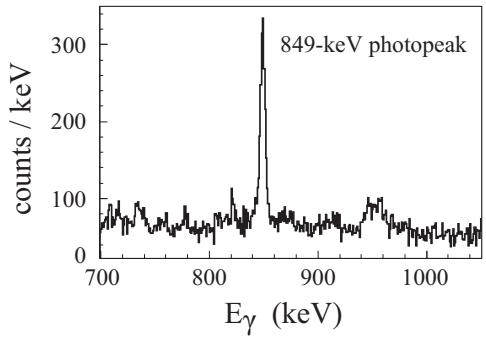

FIG. 21. A section of the ^{38}S γ-ray spectrum showing the 849-keV γ-ray photopeak. The spectrum corresponds to a sum of spectra measured at all target-degrader distances. Only one component of the photopeak is observed: that corresponding to γ-ray emission after the degrader foil.

The lifetime of the 2_1^+ state, based on a measurement of $B(E2; 0^+ \rightarrow 2^+)$ [235(30) e^2 fm^4] [71,72], is 4.8(6) ps. For the 4_1^+ state, a lifetime limit of $\tau > 0.20$ ps was established by Olness *et al.* [73] using the Doppler-shift attenuation method; states of ^{38}S were populated using the ^{36}S(t, p) reaction. To date, a direct measurement of the lifetime of the 3675-keV $J^\pi = (6^+)$ state has not been made although, as noted above, its value has previously been estimated as lying between 100 and 200 ps.

The 3675-keV $J^\pi = (6^+)$ state is relatively strongly populated in the present work, as would be expected for a yrast state. For the 849-keV photopeak, corresponding to the $(6^+) \rightarrow 4^+$ transition, only the component corresponding to γ-ray emission after the degrader is observed, see Fig. 21. It can therefore be concluded that the lifetime exceeds that which is measurable using the current recoil-distance experimental setup, namely, $\gtrsim$100 ps. The lower limit to the lifetime is in agreement with the estimate by Lunderberg *et al.* [69] made on the basis of GEANT simulations of γ-ray emission from a ^{38}S reaction residue moving with $v/c \approx 0.35$. As a consequence of the long lifetime, a measurement of the lifetimes of the 2_1^+ and 4_1^+ states would require removal of feeding from the (6_1^+) state by the application of an appropriate Q gate. Unfortunately, in this particular case, this did not prove to be possible.

From a simple shell-model perspective, the structure of the 0^+, 2^+, 4^+, and 6^+ states can be described assuming the configuration $\pi(2s_{1/2})^2 \otimes \nu(1f_{7/2})^2$, in which the two $1f_{7/2}$ neutrons couple to the required spins. As expected, the energy corresponding to the $(6^+) \rightarrow 4^+$ transition is reduced in relation to those of the two lower transitions [74]. The results of shell-model calculations based on the SDPF-U interaction show that the wave functions of the positive-parity states are mixed. The predominant component in the wave function is indeed $\pi(2s_{1/2})^2 \otimes \nu(1f_{7/2})^2$, and this contributes 54%, 37%, 40%, and 58% to the total wave function of the 0^+, 2^+, 4^+, and 6^+ states, respectively. The shell-model lifetimes of the 2^+, 4^+, and 6^+ states are 6.36, 2.89, and 64 ps, respectively, which are in relatively good agreement with the published lifetimes and lifetime limits from earlier published work [71–73] and from the present work. The corresponding transition rates are $B(E2; 2^+ \rightarrow 0^+) = 34.9$ e^2 fm^4 (4.60 W.u.), $B(E2; 4^+ \rightarrow 2^+) = 32.5$ e^2 fm^4 (4.29 W.u.), and $B(E2; 6^+ \rightarrow 4^+) = 29.0$ e^2 fm^4 (3.82 W.u.). Table IV summarizes the experimental and shell-model values of excitation energy and lifetime for the 2^+, 4^+, and 6^+ states of ^{38}S.

TABLE IV. Experimental and shell-model values of excitation energy and lifetime of excited states of ^{38}S. The quoted published lifetime for the 2^+ state is based on a measurement of $B(E2; 0^+ \rightarrow 2^+)$ [71,72], while that for the 4^+ state comes from Olness *et al.* [73].

J^π	E (expt.) (keV)	E (SM) (keV)	τ (present) (ps)	τ (previous) (ps)	τ (SM) (ps)
2^+	1292	1349		4.8(6)	6.36
4^+	2826	2426		>0.2	2.89
6^+	3675	3164	>100		64

Finally, the shell-model value of the g factor of the 2^+ state, -0.15, is in reasonable agreement with the experimental value $+0.13(5)$ [75,76], when consideration is given to the extreme sensitivity to configuration mixing and the near cancellation of proton and neutron contributions [75,76]. Here, the g factor has been evaluated using the bare nucleon g factors.

IV. CONCLUSIONS

Lifetimes and lifetime limits of excited states of the sulfur isotopes ^{35,36,37,38}S populated in binary grazing reactions were measured using the differential recoil distance method. The statistics of the γ-ray spectra corresponding to the five different target-to-degrader distances are poor and consequently the experimental uncertainties in the measured lifetimes are large. The robustness of the data analysis methodology adopted here is confirmed by the ability to reproduce known lifetimes both in the present work and in the closely related work of Grocutt *et al.* [34,35]. The measured lifetime of the first excited $J^\pi = 1/2^+$ state of ^{35}S is not particularly well reproduced in calculations which use the PSDPF interaction; it has been suggested here that this can be attributed to problems in the calculation of $M1$ transition rates, an effect which has previously been noted, see Ref. [34] and references therein. In ^{36}S, the first negative-parity state at 4193 keV with $J^\pi = 3^-$ decays to the first excited 2^+ state by an almost pure $E1$ transition. Values of $E1$ transition rates calculated using the PSDPF interaction are normally small compared with experimental values [63]; however, this is not the case here. The shell-model $B(E1)$ value is about a factor of four larger than the experimental value. Shell-model calculations within an sd-shell configuration space fail spectacularly to reproduce the experimental excitation energy of the yrast (6^+) state of ^{36}S, which is a strong indication of the importance the promotion of pairs of nucleons across the shell gap to form 2p-2h configurations. The data available here for a lifetime measurement have very poor statistics, which results in a large statistical error on the lifetime value. For the 6^+ state, calculations based on the FSU interaction are able to reproduce the experimental excitation energy to within about 500 keV, whereas sd-shell calculations result in an excitation energy approximately 9 MeV too large.

In relation to the electromagnetic decay properties of the 6^+ state, shell-model calculations based on the FSU interaction are able to reproduce the lifetime reasonably well; however, the branching ratio of the state, for which there is only a tentative experimental measurement, is poorly reproduced in the shell-model calculations. Further experimental measurements of the properties of the yrast 6^+ state would be very helpful. For the first excited $3/2^-$ and yrast $(11/2^-)$ states of ^{37}S at excitation energies of 646 and 2776 keV, respectively, lifetime limits have been established for the first time, which are in agreement with the results of shell-model calculations which employed the SDPF-U interaction. Finally, for ^{38}S, a lower limit to the lifetime of the (6^+) yrast state has been established which, while of the correct order of magnitude as the shell-model value, is nevertheless larger. Unobserved feeding from higher-lying excited states may be responsible for the difference; a measurement with significantly improved statistics would be helpful. There is good agreement between shell model and experiment for the lifetimes of the yrast 2^+ and 4^+ states. A definitive lifetime measurement of the yrast 4^+ state, rather than the current lower limit, would also be helpful in testing the shell model. The current work suffers from poor statistics. Nevertheless, lifetime values and limits have been possible, allowing a useful discussion of the ability of state-of-the-art shell-model calculations to reproduce the experimental results.

ACKNOWLEDGMENTS

The authors would like to thank the members of the AGATA collaboration for the design and development of the AGATA γ-ray tracking array used in the present experiment. The work of the team at The Institute für Kernphysik der Universität zu Köln which developed the recoil-distance differential plunger apparatus is also gratefully acknowledged. This work was supported by the UK Science and Technology Facilities Council (STFC) under Grants No. ST/L005808/1 (U.W.S.) and No. ST/P005101/1 (U.W.S.). R.S. acknowledges support through Grant No. PHY-1712953 (FSU) from the U.S. National Science Foundation, through the grant from the U.S. Department of Energy, Office of Science, Office of Nuclear Physics No. DE-SC0009883., and support from the Natural Sciences and Engineering Research Council of Canada (NSERC). T.M. and S.S. acknowledge support in part from the Croatian Science Foundation under Project No. 7194. Finally, the contribution of the accelerator and target-fabrication staff at the INFN Legnaro National Laboratory is gratefully acknowledged.

[1] A. Dewald, S. Harissopulos, and P. von Brentano, Z. Phys. A **334**, 163 (1989).
[2] A. Dewald, O. Möller, and P. Petkov, Prog. Part. Nucl. Phys. **67**, 786 (2012).
[3] S. Szilner, C. A. Ur, L. Corradi, N. Mărginean, G. Pollarolo, A. M. Stefanini, S. Beghini, B. R. Behera, E. Fioretto, A. Gadea *et al.*, Phys. Rev. C **76**, 024604 (2007).
[4] A. M. Stefanini, L. Corradi, G. Maron, A. Pisent, M. Trotta, A. M. Vinodkumar, S. Beghini, G. Montagnoli, F. Scarlassara, G. F. Segato *et al.*, Nucl. Phys. A **701**, 217 (2002).
[5] A. Gadea (EUROBALL Collaboration and PRISMA-2 Collaboration), Eur. Phys. J. A **20**, 193 (2003).
[6] R. Chapman, Z. M. Wang, M. Bouhelal, F. Haas, X. Liang, F. Azaiez, B. R. Behera, M. Burns, E. Caurier, L. Corradi *et al.*, Phys. Rev. C **93**, 044318 (2016).
[7] R. Chapman, Z. M. Wang, M. Bouhelal, F. Haas, X. Liang, F. Azaiez, B. R. Behera, M. Burns, E. Caurier, L. Corradi *et al.*, Phys. Rev. C **94**, 024325 (2016).
[8] Z. M. Wang, R. Chapman, X. Liang, F. Haas, F. Azaiez, B. R. Behera, M. Burns, E. Caurier, L. Corradi, D. Curien *et al.*, Phys. Rev. C **81**, 054305 (2010).
[9] Z. M. Wang, R. Chapman, F. Haas, X. Liang, F. Azaiez, B. R. Behera, M. Burns, L. Corradi, D. Curien, A. N. Deacon, Zs. Dombrádi, E. Farnea, E. Fioretto, A. Gadea, A. Hodsdon, F. Ibrahim, A. Jungclaus, K. Keyes, V. Kumar, A. Latina *et al.*, Phys. Rev. C **83**, 061304(R) (2011).
[10] Z. M. Wang, Ph.D. thesis, University of the West of Scotland, 2010 (unpublished).
[11] E. Caurier, G. Martínez-Pinedo, F. Nowacki, A. Poves, and A. P. Zuker, Rev. Mod. Phys. **77**, 427 (2005).
[12] H. Scheit, T. Glasmacher, B. A. Brown, J. A. Brown, P. D. Cottle, P. G. Hansen, R. Harkewicz, M. Hellstrom, R. W. Ibbotson, J. K. Jewell *et al.*, Phys. Rev. Lett. **77**, 3967 (1996).
[13] T. Glasmacher, B. A. Brown, M. J. Chromik, P. D. Cottle, M. Fauerbach, R. W. Ibbotson, K. W. Kemper, D. J. Morrissey, H. Scheit, D. W. Sklenicka *et al.*, Phys. Lett. B **395**, 163 (1997).
[14] T. R. Werner, J. A. Sheikh, W. Nazarewicz, M. R. Strayer, A. S. Umar, and M. Misu, Phys. Lett. B **333**, 303 (1994).
[15] B. Bastin, S. Grevy, D. Sohler, O. Sorlin, Z. Dombradi, N. L. Achouri, J. C. Angelique, F. Azaiez, D. Baiborodin, R. Borcea *et al.*, Phys. Rev. Lett. **99**, 022503 (2007).
[16] C. Force, S. Grévy, L. Gaudefroy, O. Sorlin, L. Cáceres, F. Rotaru, J. Mrazek, N. L. Achouri, J. C. Angélique, F. Azaiez *et al.*, Phys. Rev. Lett. **105**, 102501 (2010).
[17] X. Liang, R. Chapman, F. Haas, K. M. Spohr, P. Bednarczyk, S. M. Campbell, P. J. Dagnall, M. Davison, G. de Angelis, G. Duchene, T. Kroll, S. Lunardi, S. Naguleswaran, and M. B. Smith, Phys. Rev. C **66**, 014302 (2002).
[18] S. Go, E. Ideguchi, R. Yokoyama, N. Aoi, F. Azaiez, K. Furutaka, Y. Hatsukawa, A. Kimura, K. Kisamori, M. Kobayashi *et al.*, Phys. Rev. C **103**, 034327 (2021).
[19] S. Aydin, M. Ionescu-Bujor, G. T. Gavrilov, B. I. Dimitrov, S. M. Lenzi, F. Recchia, D. Tonev, M. Bouhelal, F. Kavillioglu, P. Pavlov *et al.*, Phys. Rev. C **96**, 024315 (2017).
[20] D. G. Jenkins, C. J. Lister, M. P. Carpenter, P. Chowdhury, N. J. Hammond, R. V. F. Janssens, T. L. Khoo, T. Lauritsen, D. Seweryniak, T. Davinson, P. J. Woods, A. Jokinen, and H. Penttila, Phys. Rev. C **72**, 031303(R) (2005).
[21] D. Tonev, G. de Angelis, I. Deloncle, N. Goutev, G. De Gregorio, P. Pavlov, I. Pantaleev, S. Iliev, M. Yavahchova, P. Bizzeti *et al.*, Phys. Lett. B **821**, 136603 (2021).
[22] D. A. Testov, A. Boso, S. M. Lenzi, F. Nowacki, F. Recchia, G. de Angelis, D. Bazzacco, G. Colucci, M. Cottini, F. Galtarossa *et al.*, Phys. Rev. C **104**, 024309 (2021).
[23] M. Bouhelal, F. Haas, E. Caurier, F. Nowacki, and A. Bouldjedri, Nucl. Phys. A **864**, 113 (2011).

[24] F. Nowacki and A. Poves, Phys. Rev. C **79**, 014310 (2009).
[25] R. S. Lubna, K. Kravvaris, S. L. Tabor, V. Tripathi, A. Volya, E. Rubino, J. M. Allmond, B. Abromeit, L. T. Baby, and T. C. Hensley, Phys. Rev. C **100**, 034308 (2019).
[26] R. S. Lubna, K. Kravvaris, S. L. Tabor. Vandana Tripathi, E. Rubino, and A. Volya, Phys. Rev. Research **2**, 043342 (2020).
[27] D. Montanari, S. Leoni, D. Mengoni, J. J. Valiente-Dobón, G. Benzoni, N. Blasi, G. Bocchi, P. F. Bortignon, S. Bottoni, A. Bracco *et al.*, Phys. Rev. C **85**, 044301 (2012).
[28] S. Bhattacharyya, M. Rejmund, A. Navin, E. Caurier, F. Nowacki, A. Poves, R. Chapman, D. O'Donnell, M. Gelin, A. Hodsdon *et al.*, Phys. Rev. Lett. **101**, 032501 (2008).
[29] C. Louchart, A. Obertelli, A. Görgen, W. Korten, D. Bazzacco, B. Birkenbach, B. Bruyneel, E. Clément, P. J. Coleman-Smith, L. Corradi *et al.*, Phys. Rev. C **87**, 054302 (2013).
[30] R. Chapman, A. Hodsdon, M. Bouhelal, F. Haas, X. Liang, F. Azaiez, Z. Wang, B. R. Behera, M. Burns, E. Caurier, L. Corradi, D. Curien, A. N. Deacon, Z. Dombradi, E. Farnea, E. Fioretto, A. Gadea, F. Ibrahim, A. Jungclaus, K. Keyes *et al.*, Phys. Rev. C **92**, 044308 (2015).
[31] R. Broda, M. Quader, P. Daly, R. Janssens, T. Khoo, W. Ma, and M. Drigert, Phys. Lett. B **251**, 245 (1990).
[32] B. Fornal, R. H. Mayer, I. G. Bearden, P. Benet, R. Broda, P. J. Daly, Z. W. Grabowski, I. Ahmad, M. P. Carpenter, P. B. Fernandez *et al.*, Phys. Rev. C **49**, 2413 (1994).
[33] I. Y. Lee, S. Asztalos, M.-A. Deleplanque, B. Cederwall, R. M. Diamond, P. Fallon, A. O. Macchiavelli, L. Phair, F. S. Stephens, G. J. Wozniak *et al.*, Phys. Rev. C **56**, 753 (1997).
[34] L. Grocutt, R. Chapman, M. Bouhelal, F. Haas, A. Goasduff, J. F. Smith, S. Courtin, D. Bazzacco, T. Braunroth, L. Capponi *et al.*, Phys. Rev. C **100**, 064308 (2019).
[35] L. Grocutt, R. Chapman, M. Bouhelal, F. Haas, A. Goasduff, J. F. Smith, S. Courtin, D. Bazzacco, T. Braunroth, L. Capponi *et al.* (unpublished).
[36] A. Dewald, in *Ancillary Detectors and Devices for Euroball*, edited by H. Grawe (GSI and the Euroball Ancillary Group, Darmstadt, 1980), p. 70.
[37] G. Montagnoli, A. M. Stefanini, M. Trotta, S. Beghini, M. Bettini, F. Scarlassara, V. Schiavon, L. Corradi, B. R. Behera, E. Fioretto *et al.*, Nucl. Instrum. Methods Phys. Res. Sect. A **547**, 455 (2005).
[38] S. Beghini, L. Corradi, E. Fioretto, A. Gadea, A. Latina, G. Montagnoli, F. Scarlassara, A. M. Stefanini, S. Szilner, M. Trotta *et al.*, Nucl. Instrum. Methods Phys. Res. Sect. A **551**, 364 (2005).
[39] A. Gadea, E. Farnea, J. Valiente-Dobón, B. Million, D. Mengoni, D. Bazzacco, F. Recchia, A. Dewald, T. Pissulla, W. Rother *et al.*, Nucl. Instrum. Methods Phys. Res. Sect. A **654**, 88 (2011).
[40] F. C. L. Crespi, F. Camera, O. Wieland, G. Benzoni, S. Brambilla, B. Million, and D. Montanari, Nucl. Instrum. Methods Phys. Res. Sect. A **570**, 459 (2007).
[41] A. Lopez-Martens, K. Hauschild, A. Korichi, J. Roccaz, and J.-P. Thibaud, Nucl. Instrum. Methods Phys. Res. Sect. A **533**, 454 (2004).
[42] B. A. Brown and W. A. Richter, Phys. Rev. C **74**, 034315 (2006).
[43] E. Caurier and F. Nowacki, Acta Phys. Pol. B **30**, 705 (1999).
[44] E. Caurier, G. Martínez-Pinedo, F. Nowacki, A. Poves, J. Retamosa, and A. P. Zuker, Phys. Rev. C **59**, 2033 (1999).
[45] W. A. Richter, S. Mkhize, and B. A. Brown, Phys. Rev. C **78**, 064302 (2008).
[46] J. Chen, J. Cameron, and B. Singh, Nucl. Data Sheets **112**, 2715 (2011).
[47] S. Aydin, M. Ionescu-Bujor, F. Recchia, S. M. Lenzi, M. Bouhelal, D. Bazzacco, P. G. Bizzeti, A. M. Bizzeti-Sona, G. de Angelis, I. Deloncle *et al.*, Phys. Rev. C **89**, 014310 (2014).
[48] W. Andrejtscheff, L. Zamick, N. Marupov, K. Muminov, and T. Muminov, Nucl. Phys. A **351**, 54 (1981).
[49] E. K. Warburton, J. W. Olness, G. A. P. Engelbertink, and T. K. Alexander, Phys. Rev. C **7**, 1120 (1973).
[50] E. Sahin, M. Doncel, K. Sieja, G. de Angelis, A. Gadea, B. Quintana, A. Görgen, V. Modamio, D. Mengoni, J. J. Valiente-Dobón *et al.*, Phys. Rev. C **91**, 034302 (2015).
[51] V. Modamio, J. J. Valiente-Dobón, S. Lunardi, S. M. Lenzi, A. Gadea, D. Mengoni, D. Bazzacco, A. Algora, P. Bednarczyk, G. Benzoni *et al.*, Phys. Rev. C **88**, 044326 (2013).
[52] N. Nica and B. Singh, Nucl. Data Sheets **113**, 1563 (2012).
[53] K.-H. Speidel, S. Schielke, J. Leske, N. Pietralla, T. Ahn, A. Costin, M. Schmid, O. Zell, J. Gerber, P. Maier-Komor *et al.*, Phys. Lett. B **659**, 101 (2008).
[54] G. Guillaume, B. Rastegar, P. Fintz, and A. Gallmann, Nucl. Phys. A **227**, 284 (1974).
[55] M. D. Rydt, M. Depuydt, and G. Neyens, At. Data Nucl. Data Tables **99**, 391 (2013).
[56] N. Stone, At. Data Nucl. Data Tables **90**, 75 (2005).
[57] N. Nica, J. Cameron, and B. Singh, Nucl. Data Sheets **113**, 1 (2012).
[58] R. Chapman *et al.* (unpublished).
[59] O. Sorlin and M. G. Porquet, Prog. Part. Nucl. Phys. **61**, 602 (2008).
[60] J. W. Olness, W. R. Harris, A. Gallmann, F. Jundt, D. E. Alburger, and D. H. Wilkinson, Phys. Rev. C **3**, 2323 (1971).
[61] A. Hogenbirk, H. Blok, M. Brand, A. V. Hees, J. V. Hienen, and F. Jansen, Nucl. Phys. A **516**, 205 (1990).
[62] E. A. Samworth and J. W. Olness, Phys. Rev. C **5**, 1238 (1972).
[63] M. Bouhelal (private communication).
[64] P. Endt, At. Data Nucl. Data Tables **55**, 171 (1993).
[65] F. Ajzenberg-Selove and G. Igo, Nucl. Phys. A **142**, 641 (1970).
[66] C. E. Thorn, J. W. Olness, E. K. Warburton, and S. Raman, Phys. Rev. C **30**, 1442 (1984).
[67] K. L. Wang, J. G. Wang, X. H. Zhou, M. L. Liu, Y. H. Qiang, S. Guo, Z. Y. Zhang, B. F. Lv, B. S. Gao, Y. H. Zhang *et al.*, Phys. Rev. C **94**, 044316 (2016).
[68] J. Chen, Nucl. Data Sheets **152**, 1 (2018).
[69] E. Lunderberg, A. Gade, V. Bader, T. Baugher, D. Bazin, J. S. Berryman, B. A. Brown, D. J. Hartley, F. Recchia, S. R. Stroberg *et al.*, Phys. Rev. C **94**, 064327 (2016).
[70] N. J. Davis, J. A. Kuehner, A. A. Pilt, A. J. Trudel, M. C. Vetterli, C. Bamber, E. K. Warburton, J. W. Olness, and S. Raman, Phys. Rev. C **32**, 713 (1985).
[71] C. Bertulani, G. Cardella, M. D. Napoli, G. Raciti, and E. Rapisarda, Phys. Lett. B **650**, 233 (2007).

[72] H. Scheit, A. Gade, T. Glasmacher, and T. Motobayashi, Phys. Lett. B **659**, 515 (2008).
[73] J. W. Olness, E. K. Warburton, J. A. Becker, D. J. Decman, E. A. Henry, L. G. Mann, and L. Ussery, Phys. Rev. C **34**, 2049 (1986).
[74] R. F. Casten, *Nuclear Structure From a Simple Perspective*, 2nd ed. (Oxford University Press, New York, 2000).
[75] A. D. Davies, A. E. Stuchbery, P. F. Mantica, P. M. Davidson, A. N. Wilson, A. Becerril, B. A. Brown, C. M. Campbell, J. M. Cook, D. C. Dinca *et al.*, Phys. Rev. Lett. **96**, 112503 (2006).
[76] A. E. Stuchbery, A. D. Davies, P. F. Mantica, P. M. Davidson, A. N. Wilson, A. Becerril, B. A. Brown, C. M. Campbell, J. M. Cook, D. C. Dinca *et al.*, Phys. Rev. C **74**, 054307 (2006).